DOKUZ EYLÜL UNIVERSITY

GRADUATE SCHOOL OF NATURAL AND APPLIED SCIENCES

POSICAST VIBRATION CONTROL OF FLEXIBLE MECHANICAL SYSTEMS

by

Ahmet Yiğit İŞLEYEN

October 2022

İZMİR

POSICAST VIBRATION CONTROL OF FLEXIBLE MECHANICAL SYSTEMS

A thesis Submitted to the
Graduate School of Natural and Applied Science of
Dokuz Eylül University
In partial Fulfillment of the Requirements for
The degree of Master of Science in Mechanical Engineering, Machine Theory and Dynamics Program

by
Ahmet Yiğit İŞLEYEN

October 2022
İZMİR

M.Sc THESIS EXAMINATION RESULT FORM

We have read the thesis entitled "**POSICAST VIBRATION CONTROL OF FLEXIBLE MECHANICAL SYSTEMS**" completed by **Ahmet Yiğit İŞLEYEN** under supervision of **PROF.DR. LEVENT MALGACA** and we certify that in our opinion it is fully adequate, in scope and in quality, as a thesis for the degree of Master of Science.

....

Prof. Dr. Levent MALGACA

Supervisor

....

Prof. Dr. Hasan ÖZTÜRK

(Jury Member)

....

Assoc. Prof. Dr. Mehmet İTİK

(Jury Member)

Prof. Dr. Okan FISTIKOĞLU

Director

Graduate School of Natural and Applied Sciences

ACKNOWLEDGEMENTS

First of all, I would like to thank Prof. Dr. Levent MALGACA, my advisor, whose guidance, constructive suggestions and continued interest were vital to the completion of this work. It is really chance to study under his supervision.

I wish to express my gratitude to Res. Assist. Seda Vatan Can who assisted me to carry out my studies in the large scale at Dokuz Eylül University.

Ahmet Yiğit İŞLEYEN

POSICAST VIBRATION CONTROL OF FLEXIBLE MECHANICAL SYSTEMS

ABSTRACT

Posicast control method is an input shaping method used in oscillatory systems. The posicast control method can be applied to feedforward and feedback systems. The feedforward posicast control requires the open-loop system while the feedback posicast control requires the closed-loop system. Inputs can be shaped by applying the posicast methods to open-loop and closed-loop systems.

In this thesis, the feedforward posicast method is studied by shaping the inputs. The lumped-parameter mechanical systems as single-degree-of-freedom (S-DOF) and multi-degree-of-freedom (M-DOF), and a single-link flexible manipulator are considered. The step and trapezoidal inputs are shaped using the half and three-step posicast methods.

The half-cycle has a single amplitude and delay time while three-step cycles have three amplitudes and two delay time parameters. The shaped amplitude and delay time parameters are calculated by using the undamped natural frequency and damping ratio of the considered system. Simulations are carried out by MATLAB for the S-DOF and M-DOF systems, and ANSYS for the manipulators. The shaped inputs are also prepared by MATLAB. The time responses and tabulated results were presented in order to compare the performances of uncontrolled and controlled cases.

Keywords: Posicast control, vibration suppression, input shaping, open-loop

ESNEK MEKANİK SİSTEMLERİN POSICAST TİTREŞİM KONTROLÜ

ÖZ

Posicast kontrol yöntemi, salınımlı sistemlerde kullanılan bir girdi şekillendirme yöntemidir. Posicast kontrol metodu ileri-besleme ve geri-besleme sistemlerine uygulanabilir. İleri-besleme posicast kontrolü bir açık-çevrim sistem gerektiriyorken, geri-besleme posicast kontrolü kapalı-çevrim bir sistem gerektirir. Girdiler açık-çevrim ve kapalı-çevrim sistemlere uygulanarak şekillendirilebilirler.

Bu tezde, girdiler şekillendirilerek, ileri-besleme posicast kontrolü çalışılmıştır. Sistemler olarak toplu-parametreli sistemler olan tek-serbestlik-dereceli ve çok-serbestlik-dereceli sistemler, ayrıca tek-uzuvlu esnek bir manipülatör ele alınmıştır. Yarım ve üç-adımlı posicast çevrimi kullanılarak adım ve trapezoidal girdiler şekillendirilmiştir.

Yarım-çevrim posicast iki genlik ve bir gecikme zamanı içeriyorken, üç-adımlı posicast çevrimi üç genlik ve iki gecikme zamanından oluşur. Şekillendirilmiş genlik ve gecikme zamanı parametreleri ilgili sistemin sönümsüz doğal frekansı ve sönüm oranı kullanılarak hesaplanır. Simulasyonlar tek-serbestlik ve çok-serbestlik-dereceli sistemler için MATLAB’da, manipülatör için ANSYS’te gerçekleştirilmiştir. Şekillendirilmiş girdiler ayrıca MATLAB’da hazırlanmıştır. Kontrol uygulanmış ve uygulanmamış durumların performanslarını karşılaştırmak için zaman cevapları ve tablolanmış sonuçlar sunuldu.

Keywords: Posicast kontrol, titreşim sönümleme, girdi şekillendirme, açık çevrim

CONTENTS

Page

LIST OF FIGURES

Page

LIST OF TABLES

Page

LIST OF SYMBOLS

ω_n	: Undamped Natural Frequency
ω_d	: Damped Natural Frequency
ζ	: Damping Ratio
e	: Exponential Constant
A_1	: Initial Amplitude
A_2	: Second Amplitude
A_3	: Third Amplitude
T_1	: Initial Delay (Transition) Time
T_2	: Second Delay (Transition) Time
T_3	: Third Delay (Transition) Time
T_d	: Damping Time Period
t_p	: Initial Peak Time
P(s)	: Posicast Control Equation In s-domain
δ	: Overshoot
ov	: Overshoot (letter form of δ)
$G_{hc}(s)$	: Transfer Function Of Half-Cycle Posicast Controller
$G_{ts}(s)$	: Transfer Function Of Three-step Cycle Posicast Controller
F	: External Force
m	: Mass Of S-DOF System
c	: Damping Constant Of S-DOF System

k : Spring Constant Of S-DOF System

m_i : ith Mass Of M-DOF System

c_i : ith Damping Constant Of M-DOF System

k_i : ith Spring Constant Of M-DOF System

x : Displacement

$\dot{x}$: Velocity

$\ddot{x}$: Acceleration

$H(s)$: Transfer Function Of S-DOF System

$H_{41}(s)$: Transfer Function Of M-DOF System

$D_{41}(s)$: Characteristic Equation Of Input For M-DOF System

Θ : Angle Of Between Real Axis And Resultant Vector

ω_0 : Maximum Angular Velocity

t_{acc} : Acceleration Time

t_{con} : Constant Velocity Time

t_{dec} : Deceleration Time

TM-1 : Motion Profile-1

TM-2 : Motion Profile-2

CHAPTER ONE

INTRODUCTION

From the past to the present, technology has existed to discover and advance industrial research in our lives at substantial level. Manipulators are significant systems of this technology which transport a specific component from a point to another point. During this transportation, vibrations occur that cause reducing motion accuracy. Thus, the vibrations must be eliminated or reduced. Vibration control methods must be employed to eliminate vibrations. These systems are able to modelled as single or multi-degree-of-freedom system depending on number of the lumped-parameter systems. These control methods can be classified as active and passive controls. If extra materials are utilized such as sensors and actuators in a vibration control process, this method is an active control. In addition, an active control is required a real-time tracking situation. On the other hand, if a vibration control process is not required an extra material or a real-time tracking situation, this control method is a passive vibration control.

Some passive vibration control methods are given. Passive vibration control is applied to a thin-walled composite beam (Rimašauskienė, Jūrėnas, Radzienski, Rimašauskas & Ostachowicz, 2019). Two permanent cuboidal magnets are used for performing the passive vibration control. The magnets are attached to end-point of the beam. Vibration is created via macro fibre composite MFC that is located on the beam. It is provide that the magnets approach to each other, thereby the residual vibration is eliminated, experimentally. Rotor system is investigated in terms of reducing residual vibration (Ribeiro, Pereira & Bavastri, 2015). Passive vibration control is applied to the rotor system. The control method is determined as viscoelastic elements. The elements are added equation of motion of the rotor. This process is realized by using degree-of-freedom and generalized equivalent parameters GEP technique. Undesirable vibrations and transmissibility are decreased with the passive vibration control. A beam is exposed to passive vibration control (Younesian, Esmailzadeh & Sedaghati, 2006). The beam is designed by Timoshenko beam theory. The controller is optimal tuned mass damper TMD for eliminating vibrations. The results of the system are shown as root mean square RMS values and experimentally. The passive control technique has up to 55% and 42% eliminating reducing for undamped beam and damped beam, respectively. Passive vibration control is determined by designing multiple tuned mass dampers TMDs (Tong & Zhao, 2018). The controller is applied to nonuniform spacecraft control laboratory experiment beam system NASA SCOLE system. TMD system is realized an efficient performance compared to conventional methods that are obtained from Den Hartog and Warburton's formulations. On the other hand, TMD system is suppressed multi-dominant vibrations simultaneously. It is observed that the multiple tuned mass dampers give good results compared to single tuned mass damper in terms of robustness and effectiveness. A passive vibration control is applied to a SCARA robot arm (Tang, Pan & Cheng, 2019). The arm has a high deformation because of vibration. The controller is determined by changing shape of base of the arm. The unshaped arm has two squares base. The base is altered with a circular base. Thereby, the arm has more contact surface. Thus, stress and deformation vibration are eliminated. Posicast control method is a passive control method.

In this study, posicast control method is investigated for flexible manipulators as the lumped-parameter models. The posicast control method is classified as feedforward posicast studies, feedback posicast studies and both of feedforward and feedback posicast studies in this section. The feedforward posicast method is a pre-filter design. This method is located open-loop section and out of feedback section. The feedback posicast is a method that is located within a feedback loop. The feedforward posicast is converted to feedback posicast method (Hung, 2007). More robust results are obtained owing to the within feedback posicast method compared to the feedforward type. The control method is studied as half-cycle posicast. On the other hand, the method is developed as three-step cycle posicast. This type has three amplitudes and two delay time factors.

Many researchers study on power converters, slewing structures, satellite system, servo systems, second or higher-order systems as modelled a transfer function and so on by applying the posicast control method. This paragraph contains both of feedforward and feedback posicast studies. The posicast method is investigated as chronological sequence in terms of development of posicast method by Hung (Hung, 2007). In general, Hung states that firstly, the posicast method is studied as feedforward posicast. Then the posicast method is converted to feedback posicast for higher damping quality and decreasing sensitivity problems. The posicast control method is extended from two fractional form to three fractional form by adding PID controller to higher-order oscillatory systems by Oliveira, Vrancic and Cunha (Vrancic, Cunha & Oliveira, 2012). The proposed method is taken place as feedforward posicast, feedback posicast and dual mode posicast configurations. The researchers are cancelled undesirable overshoot value and decreased settling time as experimental results.

The other feedforward and feedback studies are shown in this paragraph. Hung is realized a comparison between feedforward and feedback posicast control as performance of damping (Hung, 2003). A buck-type dc-dc voltage converter is employed as the system. The input shaping method is studied as theoretical and experimental analysis. The researcher referred that the feedback posicast demonstrated suppression precisely compared to the feedforward posicast. The posicast control is classified as the feedforward posicast and the feedback posicast (Emmanuel A. Gonzalez, 2007). Gonzalez is analized power converter systems. The posicast control method produces efficient responses. The method can be implemented in discrete-time hardware, purely. High frequency noises are reduced significantly compared to PID controller. These results are obtained as experimentally. The posicast control method can be applied to eliminate multi-unadapted frequency intervals as staggered posicast form (R. A. Fowell, 1997). The method is applied to satellite control systems. The posicast method is staggered form and located in open-loop and feedback sections without coinciding to each other. The proposed method mitigates to undesirable resonance effects. The advantage of the input shaping method is ability of the applying instantly for the actuators. The posicast control method has been succeed eliminating undesired resonance effect in unstabil frequency interval.

The feedforward posicast method is investigated in this paragraph. The two fractional posicast method is employed by Oliveira and Vrancic (Oliveira & Vrancic, 2012). The researchers examined the half-cycle posicast method as a feedforward compensator on underdamped second-order systems for increase tracking performance. Proportional-Integral-Derivative PID controller was employed for eliminating disturbance effect. The study is realized experimentally. The posicast method is illustrated a robust set-point tracking performance rather than PID controller. The one-quarter cycle posicast is studied by Smith as the feedforward posicast form. (Smith, 1957). The researcher studied the posicast control on a load compensator system as lightly damped feedback system as experimentally. The three-step posicast is consisted of non-minimum phase components. However, the proposed method is consisted of a minimum phase as an entire construction. Thus, the method is carried out an efficient damping quality.

The feedforward posicast studies continue in this paragraph. The posicast control method as pre-filter design is compared to a conventional types of compensation by Cook (G. Cook, 1962). The conventional type systems are based on feedback control systems. The researcher proposes the posicast method because of eliminating the resonant peak and the overshoot. The feedforward posicast method is utilized as half-cycle posicast with particle swarm optimization PSO algorithm, experimentally (J. Oliveira, P. M. Oliveira, T. M. Pinho & J. Boaventura-Cunha, 2017). Second-order feedback control systems are analized as the systems. Proportional-Integral-Derivative PID controller is employed for disturbance rejection. The posicast method is created a certain set-point tracking quality. The proposed method is utilized as open-loop feedforward design (P.B.M. Oliveira, E.J.S. Pires, & P. Novais, 2015). Two-degrees-of-freedom control configuration is designed as the feedback system.

Proportional-Integral-Derivative PID controller is determined as the feedback controller. The posicast method is succeed an efficient set-point tracking and disturbance rejection compared to PID controller.

The feedback posicast method is illustrated in this paragraph. The proposed method is applied to a fourth-order system rather than a second-order system with the half-cycle posicast by Cook as the feedback posicast (G. Cook, 1966). The author claims that the proposed method is an appropriate controller for the second-order systems. However, Cook demonstrates that the posicast method is an entirely efficient system for the fourth-order system. A tracking radar antenna is used as the fourth-order system and analized via analog computer simulation. The posicast control is reduced overshoot and cancelled resonant peaking. The feedback posicast method is applied second and higher-order systems as experimentally (H. C. So & G. J. Thaler, 1960). Firstly, the method is studied on a second-order system. Then, a feedback is added for more robust damping and decreasing load disturbances. The tapped delay line is used for higher-order systems as third and fourth-order systems. The fourth-order system is examined as a positioning servo system as a physical system. The second and third-order systems are investigated as computer simulations. The posicast control method is obtained desirable damping quality without altering features of the systems.

The other feedback posicast studies are mentioned in this paragraph. The researchers evaluate the flexible systems in terms of delay-based input shapers and one of the shapers is the posicast control method (Kucera V. & Hromcik M., 2011). This control method is integrated within feedback systems by using Smith predictor form. A positioning servo with an attached flexible beam is examined as the system. The results are obtained as experimentally. The input shaping method realizes reducing vibrations and eliminating disturbance effect.

On the other study, the feedback posicast method is proposed to suppress undesirable vibrations for the excitation and automatic voltage regulator AVR systems (A. Ghorbani, S. Pourmohammad & M. S. Ghazizadeh, 2008). Simulations are determined as experimentally. Researchers argue that the altered reference signals of the systems are caused residual oscillations. The posicast method is realized some substantial benefits for decreasing overshoot and settling time. The feedback posicast method has a robust construction to mitigate sensitivity problem compared to the feedforward posicast.

The other feedback posicast method studies are given in this and next paragraphs. The feedback posicast method is applied to the excitation and automatic voltage regulator AVR systems in the wind farm as experimentally (H. Ghorbani, J. I. Candela, A. Luna & P. Rodriguez, 2014). The proposed method is eliminated the undesirable vibrations. When novel load is also added to the system, the posicast method protects its damping quality. Therefore, the posicast method proves that is an adaptive control method. The feedback posicast is determined to cancel overshoot and create proper settling time. Also, the proposed posicast form is determined to reduce sensitivity based on feedforward posicast (Kalantar S. M. & Mousavi G., 2010). The researchers is utilized single-ended primary-inductor converter SEPIC based on DC-DC converter as the system as experimentally. PID controller is applied. The feedback posicast is damped the noise effect, while PID controller is not damping the noise effect.

The feedback posicast method is investigated in a synchronous generator connected through two parallel transmissions lines experimentally. (M. R. Aghamohammadi, A. Ghorbani & S. Pourmohammad, 2008). Voltage values changes in the generator. This changing of the voltage causes to mitigate robust of the generator. The proposed method is realized cancelling of the changing and voltage stability. The feedback posicast method eliminates the overshoot and the settling time of the signal to the generator field windings.

Feedback posicast method studies are continued in this and next paragraphs. The feedback posicast control method is compared to the empirical phase-shift controller (Park, S., Wee, D., Annaswamy, A. M., & Ghoniem, Ahmed F. 2002). The posicast control is employed for a combustor test-rig model. The researchers prove that the posicast control method is carried out suppressing pressure oscillations in substantial level compared to the empirical phase-shift controller. In addition, the experiment is verified that the posicast control method has a capable of stabilizing. The proposed method is examined as feedback posicast form theoretically and experimentally. (Q. Feng, J. Y. Hung, & R. M. Nelms, 2003). The posicast control method is applied to a boost converter that is nonlinear and lightly damped system. The proposed controller design succeeds to eliminate sensitivity problems compared to the classical posicast, substantially. Also, right half plane RHP zero of the system causes undesirable affects for some feedback controllers, but the feedback posicast is not effected. The proposed method is realized a superior damping quality in the boost converter.

The feedback posicast control method is applied by Feng, Nelms and Hung experimentally (Q. Feng, R. M. Nelms, & J. Y. Hung, 2006). The posicast method is evaluated for a buck dc-dc converter system. The proposed technique is also compared to the proportional-integral-derivative PID controller. The posicast control method is ensured that has a lower gain margin in high frequency compared to PID controller. Thus, the proposed method is realized reducing noise effect than PID controller. In addition, the proposed technique is succeeded to eliminating the overshoot in the system and cancelled sensitivity. The posicast method has a superior damping quality. PID controller is required extra modifications, but the posicast method is not required. Sugiki and Furuta are defined the feedback posicast control with internal model control design as the finite-time settling control (Sugiki A. & Furuta K., 2006). The proposed method is realized a perfect precision control for uncertain plants. On the other hand, the researchers advocate that the posicast method can exist a quick response in the systems. Also, the posicast method is realized high sensitivity to model uncertainity. The proposed method is an appropriate input shaper as within a feedback-loop to obtain dead-beat response

(Tallman G. H & Smith O. J. M., 1958). The authors express that the proposed control method is enabled for a lightly damped servomechanism system. The posicast control method suppress the vibrations and cancels the overshoot. The proposed method has an excellent waveform and simple applying feature. The researchers propose time-delayed input shapers for slewing structures. (Singh T. & Singhose W., 2002). This study is included real-time shaping or time-delay filtering to realize maneuvering ability such as posicast method in minimum time. The adaptive posicast control is considered for an engine fuel-to-air ratio control in gasoline engines (Yildiz Y., Annaswamy A., Kolmanovsky I. & Yanakiev D., 2010). In the proposed method, the Lyapunov-Krasovskii function is employed. The posicast control method is substantial valid in terms of developing the closed-loop performance.

In this pharagraph, the other vibration control methods are given for a lumped-parameter system and single-link manipulators except the posicast control method. Vibration control is applied to a single-link planar and a curved manipulator (Malgaca, Yavuz, Akdağ & Karagülle, 2016). The manipulators are modelled with finite element method FEM. The vibrations response is simulated by ANSYS and experimentally. In addition, Newmark method is used for analyzing the results. Newmark method verifies results in the planar manipulator. For the curved manipulator, Newmark method is not confused. The residual vibrations of the manipulators are eliminated by determining suitable deceleration times. On the other study, a flexible robot arm is considered a four-degree-of-freedom system (Yavuz, Malgaca & Karagülle, 2016). Closed-loop active vibration control is applied to the system. Numeric solutions are adapted in Newmark method. Numerical and analytical results give desirable solutions with Newmark method. The active vibration control reduce undesirable vibrations.

In this thesis, the posicast control method is applied to the lumped-parameter systems and a planar manipulator as open-loop. Firstly, the half-cycle is investigated. Then, the three-step cycles are studied. It is observed that the three-step cycles have different damping qualities between each other. These differences are shown with graphs and illustrated with root mean square RMS and settling time values.

The originality of the study is comparing damping quality of the three-step cycles. In addition, the vectorial analysis are identified. The lumped-parameter systems and a planar manipulator are modelled to implement posicast control.

CHAPTER TWO

THEORY OF POSICAST CONTROL

Posicast control is a passive control method to cancel vibrations based on input shaping method. The input shaping method generates zero vibration by using a second delayed impulse according to the response of a system as an impulse input. In this thesis, step input profile and trapezoidal input profile are employed. The step input is utilized for theoretical defining. On the other hand, the trapezoidal motion input is applied to the system in Section 4.

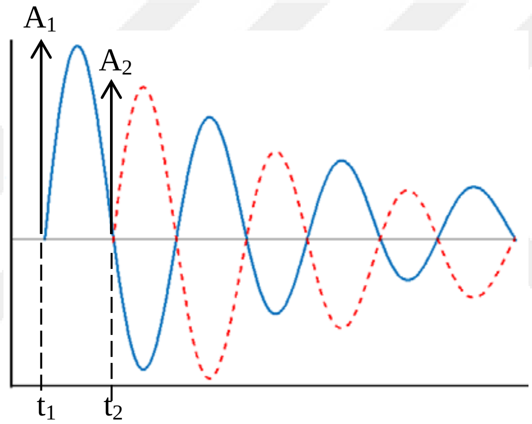

Figure 2.1 Position responses of the two sequintial impulses

A_1 is an initial impulse acted on a system at t_1. This impulse causes the oscillation of the system on its damped natural frequency. After that, the second impulse A_2 is applied to eliminate the residual vibrations after the initial impulse as shown in Figure 2.1. The residual vibration formula is shown below:

$$V(\omega,\zeta) = e^{-\zeta\omega t_n}\sqrt{C(\omega,\zeta)^2 + S(\omega,\zeta)^2} \tag{2.1}$$

The $C(\omega,\zeta)$ and $S(\omega,\zeta)$ are the phasors of free vibrations and equal to zero to obtain zero residual vibration. Equation (2.1) determines by taking rate of the free vibrations.

$$C(\omega,\zeta) = \sum_{i=1}^{n} A_i e^{\zeta\omega t_i}\cos(\omega_d t_i) \tag{2.2}$$

$$S(\omega,\zeta) = \sum_{i=1}^{n} A_i e^{\zeta\omega t_i}\sin(\omega_d t_i) \tag{2.3}$$

A_i and t_i are the amplitudes and time values. ω, ω_d and ζ are undamped natural frequency, damped natural frequency and damping ratio parameters, respectively. In addition, n defines as number of impulses. If the initial amplitude A_1 is applied at the initial time that is zero, t_1 equals to zero as shown in Figure 2.1. Equations (2.2) and (2.3) equal to zero:

$$A_1 + A_2 e^{\zeta\omega t_2}\cos(\omega_d t_2) = 0 \tag{2.4}$$

$$A_2 e^{\zeta\omega t_2}\sin(\omega_d t_2) = 0 \tag{2.5}$$

Sine expression should be zero, because of nontrivial solution. Thus, the second time value can be defined as:

$$\omega_d t_2 = m\pi \tag{2.6}$$

$$t_2 = \frac{m\pi}{\omega_d} = \frac{mT_d}{2} \tag{2.7}$$

In equation (2.7), T_d is the damped time period. Moreover, if the amplitudes of the impulses have not a constraint situation, the equation (2.1) is infinite or zero that is an undesirable solution. However, if sum of the amplitudes is considered to one due to unity impulse, the equation has a desirable solution. Sum of the amplitudes is:

$$\sum A_i = 1 \tag{2.8}$$

Equation (2.4) has two fractional form. If the amplitudes of the two fractional form are computed for the minimum t_2, the relation is given with respect to equation (2.8). t_2 is the delay time acted on the second impulse. We obtain:

$$A_1 - (1 - A_1)\exp\left(\frac{\zeta\pi}{\sqrt{1-\zeta^2}}\right) = 0 \tag{2.9}$$

$$A_1 = \frac{\exp(\frac{\zeta\pi}{\sqrt{1-\zeta^2}})}{1+\exp(\frac{\zeta\pi}{\sqrt{1-\zeta^2}})} \qquad A_2 = \frac{1}{1+\exp(\frac{\zeta\pi}{\sqrt{1-\zeta^2}})} \tag{2.10}$$

When these two impulses are employed with the minimum t_2 given as equation (2.9), this method is half-cycle posicast. In addition, more amplitudes can be added to the posicast control. This process is investigated in Section 2.2.

2.1 Half-Cycle Method

Posicast control aims to complete its action at least time. The posicast control deals with the roots of the system to eliminate complex pair of poles that causes residual vibrations. The input shaping method must be employed minimum t_2 as given in equation (2.7). Thus, m equals to 1 and the second delay time t_2 is $T_d/2$. This time parameter is half of the damped time period T_d. This posicast form is the half-cycle posicast.

The posicast method is associated with a fishing rod mechanism. The fishing rod mechanism is thrown to target point in the sea. The mechanism arrive to target point after a delayed time. After that, it has a zero velocity, suddenly. The posicast method is realized zero velocity by applying a second amplitude acted on a delayed time. Thus, the posicast method is entitled to positive-cast control (Smith, 1957). The posicast control is demonstrated on a pendulum system in Figure 2.2 (Hung, 2003):

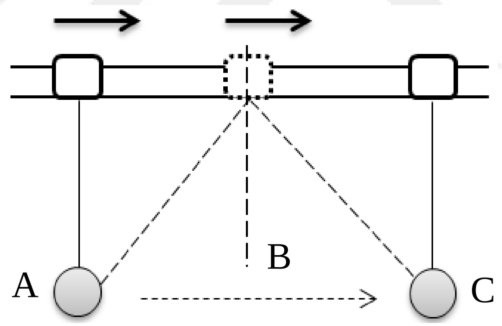

Figure 2.2 Principle of the posicast control for a pendulum mechanism

The system is a pendulum as given in Figure 2.2. Support that is connected to a ball via a rope is placed on the gantry. The ball acts on the gantry by applying an input force in the horizontal trajectory. First of all, the support stays at the rest position in region A. Then, it is moved from starting point under the first instant impulse A_1. The support arrives mid-point of the gantry in region B. When the support reaches the mid-point, the ball starts to oscillation with an angular trajectory from the starting point A. When the ball realizes its angular trip up to maximum distance in region C, the support is moved with the second instant pulse A_2 from its position to the final position as shown in region C. In the end, the payload is submitted final position without residual vibration by this half-cycle posicast method. The half-cycle formulation is given in Equation (2.12) (Hung, 2007). P(s) and $G_{hc}(s)$ represent the posicast and the half-cycle posicast expressions in Equations (2.11) and (2.12). δ is the overshoot as shown in Figure 2.3. Transfer function of the half-cycle posicast is given in Equation (2.13).

$$P(s) = \frac{\delta}{1+\delta}\left[-1 + e^{-s\left(\frac{T_d}{2}\right)}\right] \tag{2.11}$$

$$G_{hc}(s) = 1 + P(s) \tag{2.12}$$

$$G_{hc}(s) = A_1 + A_2 e^{-\frac{T_d}{2}s} \tag{2.13}$$

$$A_1 = \frac{1}{1+\delta} \quad A_2 = \frac{\delta}{1+\delta} \tag{2.14}$$

$$\delta = e^{\frac{-\zeta\pi}{\sqrt{1-\zeta^2}}} \tag{2.15}$$

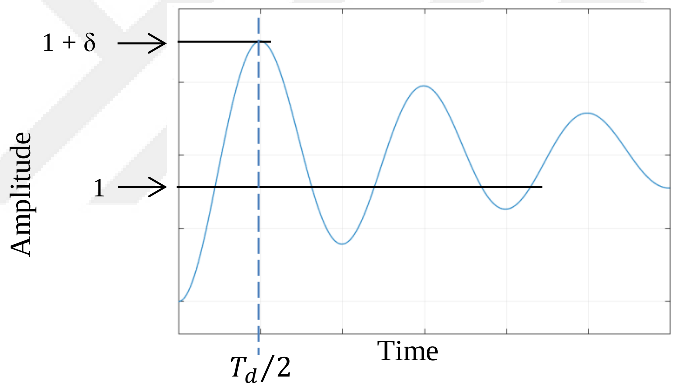

Figure 2.3 Response of A_1 impulse

This method which is developed based on impulse signals is also applied to various input forms. For instance, if the half-cycle method is applied to a step input given in Figure 2.4, the shaped signal is obtained in Figure 2.5.

The half-cycle posicast is able to demonstrate in two case in terms of block diagram form (Hung, 2003):

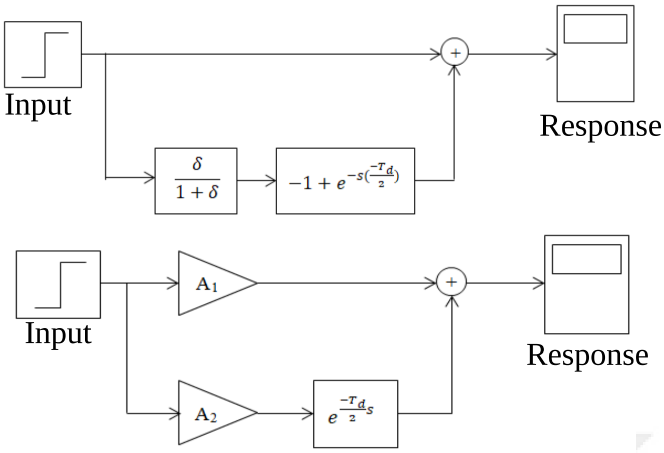

Figure 2.4 Two configurations of the half-cycle posicast

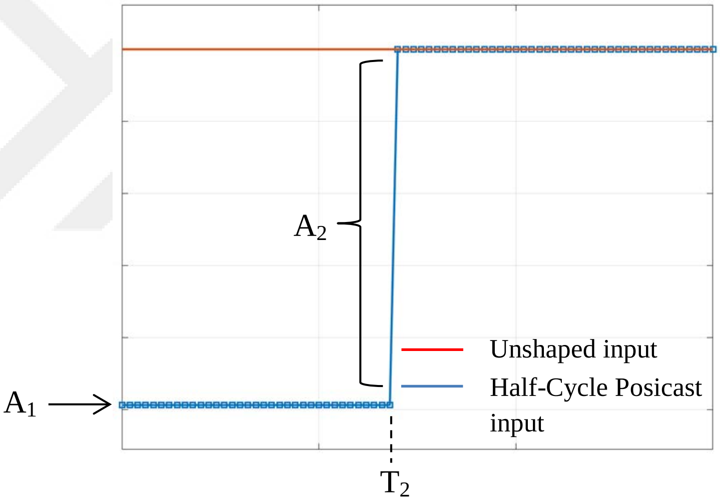

Figure 2.5 Unshaped step input and the half-cycle posicast step input signals

The half-cycle method is performed its input signal as two fractional signal. However, if the number of the amplitudes are three, the input signal is shown in Section 2.2 as Laplace transform.

2.2 Three-step Cycle Method

The three-step cycles define by adding one more delayed amplitude and as equation (2.16) (Oliveira, Vrancic and Cunha, 2012):

$$G_{ts}(s) = A_1 + A_2 e^{-T_2 s} + A_3 e^{-T_3 s} \tag{2.16}$$

If input signal is a unity impulse input, sum of the amplitudes is one shown as equation (2.8).

$$A_1 + A_2 + A_3 = 1 \tag{2.17}$$

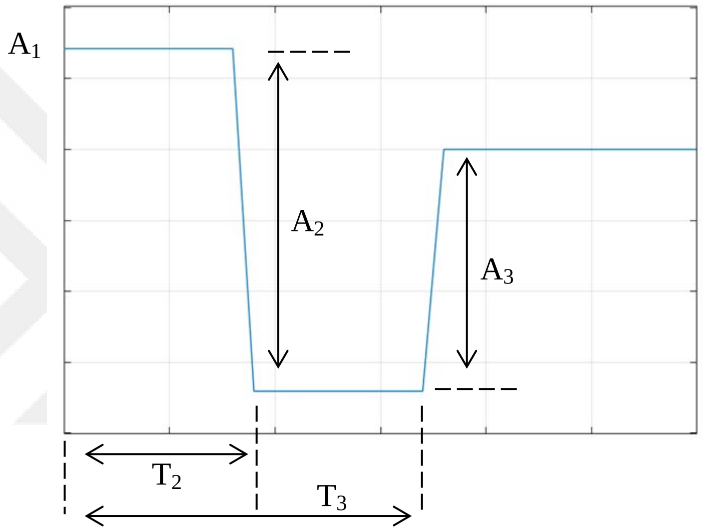

Figure 2.6 One-quarter cycle posicast graph

In Figure 2.6, the three amplitudes and the delay times are shown for the one-quarter cycle form as an instance. The three-step cycle equation is given (Oliveira, Vrancic & Cunha, 2012):

$$A_1 + A_2 e^{-T_2 s} + A_3 e^{-T_3 s} = 0 \tag{2.18}$$

$$A_1 + A_2 e^{-\sigma T_2} \cos(\omega T_2) + A_3 e^{-\sigma T_3} \cos(\omega T_3) = 0 \tag{2.19}$$

$$A_2 e^{-\sigma T_2} \sin(\omega T_2) + A_3 e^{-\sigma T_3} \sin(\omega T_3) = 0 \tag{2.20}$$

$$\sigma = -\xi \omega_n \tag{2.21}$$

$$\omega = \omega_d \tag{2.22}$$

As expressed above, the amplitude formulations are found by taking as equations (2.2) and (2.3). The amplitudes can be computed as shown equations (2.23), (2.24) and (2.25).

$$A_1 = \frac{e^{2\xi\omega_n T_2}}{1-2e^{\xi\omega_n T_2}\cos(\omega_d T_2)+e^{2\xi\omega_n T_2}} \tag{2.23}$$

$$A_2 = \frac{-2e^{\xi\omega_n T_2}\cos(\omega_d T_2)}{1-2e^{\xi\omega_n T_2}\cos(\omega_d T_2)+e^{2\xi\omega_n T_2}} \tag{2.24}$$

$$A_3 = \frac{1}{1-2e^{\xi\omega_n T_2}\cos(\omega_d T_2)+e^{2\xi\omega_n T_2}} \tag{2.25}$$

Three-step posicast method has different types change with the delay time values. T_1 equals to zero. T_2 and T_3 expressions represent the first and second delay times, respectively. The delay times employ as $T_3=2T_2$. If $T_2=T_d/2$ and $T_3=T_d$, the cycle is one-cycle posicast. In the higher cycle posicast, T_2 determine with $T_d/2i$ for one-ith cycle posicast where $i>=2$. For instance, T_2 equals $T_d/6$ in one-third cycle posicast. Input signals of the half-cycle posicast and three-step cycle posicast are given in Figure 2.7:

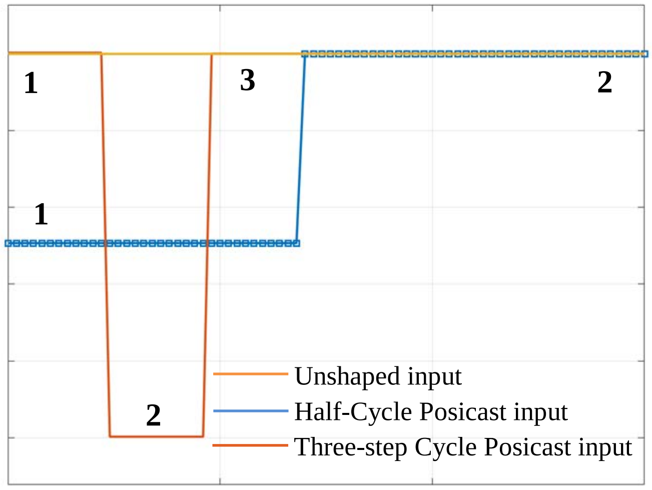

Figure 2.7 Half-cycle and three-step cycle posicast step input signals

The principle of three-step cycle input signal is illustrated with vectorial analysis:

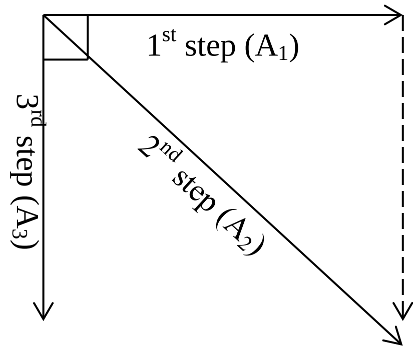

Figure 2.8 Vectorial analysis of the one-quarter cycle posicast

For instance, if the one-quarter cycle posicast is investigated, the amplitudes are demonstrated given in Figure 2.8. The vectorial sum of these vectors are zero.

A generalized isosceles perpendicular triangle is given in Figure 2.9. k is a constant for a vertical edge. When the vertical edge is computed as k, the non-vertical edge is equivalent multiply of $\sqrt{2}$:

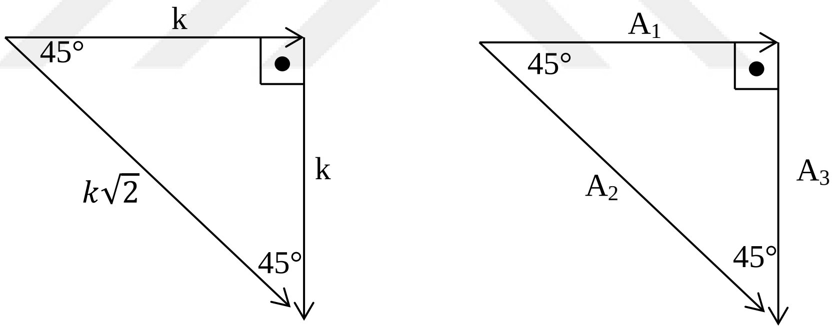

Figure 2.9 Relationship of perpendicular triangle and one-quarter cycle posicast

As shown in Figure 2.9, the triangle and the formulation are demonstrated consistent results. The negative second step is given in Figure 2.10:

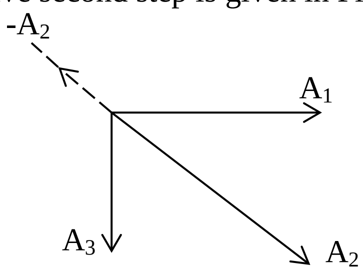

Figure 2.10 Position of the second step in negative sign

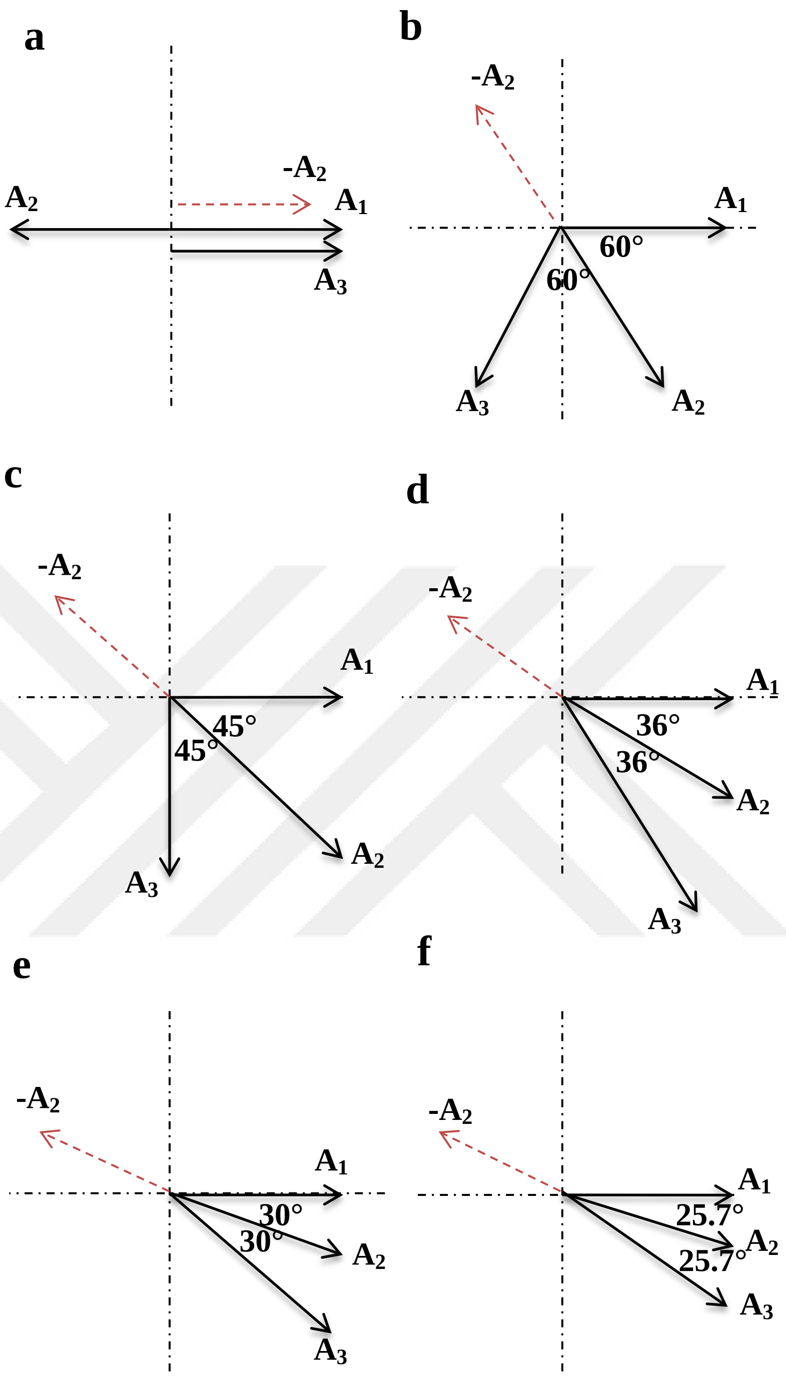

Figure 2.11 Vectorial analysis of the posicast control method (**a** one-cycle, **b** one-third cycle, **c** one-quarter cycle, **d** one-fifth cycle, **e** one-sixth cycle, **f** one-seventh cycle)

In Figure 2.11, the posicast control method is demonstrated as the vectorial analysis in the three fractional form (Smith, 1957).

In the three-step posicast, the second amplitude is a braking force. Thus, this amplitude has a negative sign. Dashed line that is the braking force is illustrated on reverse way as shown in Figure 2.11. The block diagram of the three-step cycle is given in Figure 2.12:

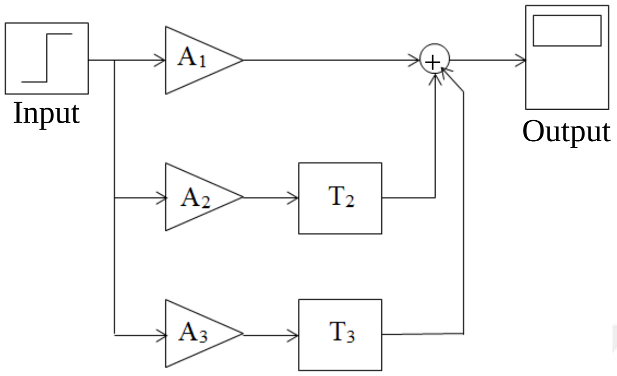

Figure 2.12 Block diagram form for the three-step cycle posicast in SIMULINK

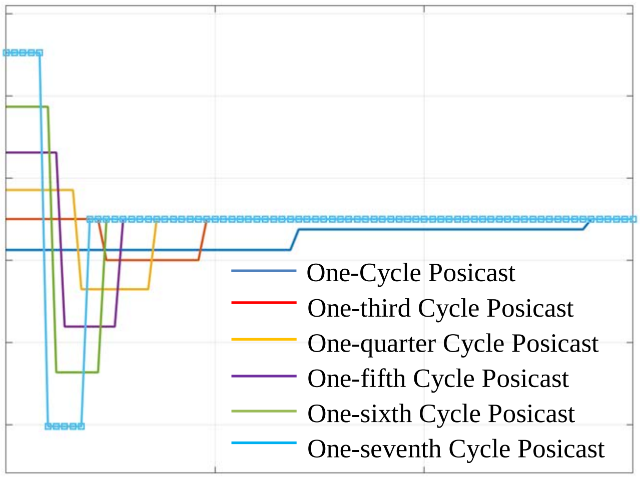

Figure 2.13 Step input signals of the three-step posicast cycles

In Figure 2.13, the step input signals of the three-step posicast cycles are demonstrated. In the posicast control method is considered in terms of the delay time factor and vibration magnitude, while the vibration magnitudes are decreasing, the delay times increase toward clockwise given as Figure 2.11. However, the vibration magnitudes increase and the delay times decrease for counter-clockwise. Note that, this comparing of vibration magnitude and the delay time are considered compared to between the three-step posicast cycles.

CHAPTER THREE

MODELLING OF MECHANICAL SYSTEMS

3.1 The Single-Degree-Of-Freedom System

In this section, a manipulator is considered as an equivalent mass-spring-damper system which is a single-degree-of-freedom (S-DOF). The S-DOF system is shown in Figure 3.1.

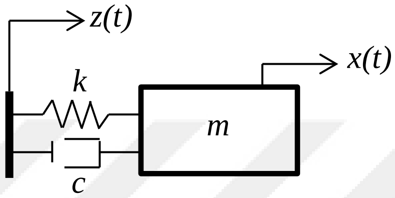

Figure 3.1 Single-degree-of-freedom system

The spring-mass-damper system is realized vibration under an effect of input *z(t)*.

In Equation (3.1), the equation of motion of S-DOF system is obtained:

$$m\ddot{x} + c\dot{x} + kx = z(t) \tag{3.1}$$

where, *z(t)*, *m*, *a*, *x*, *c* and *k* expressions are the ground forced corresponding to time as an input, the mass, acceleration, displacement, damping and spring constants, respectively. When a force or an input is applied, vibrations occur in the system. The vibrations are analyzed through transfer function of the system. As given in Equation (3.2), the differential equation converts to characteristic equation by Laplace transform. Therefore, the converted equation is defined as the transfer function as given in Equation (3.3). The transfer function is found by taking ratio the system output of the Laplace transform to the system input of the Laplace transform:

$$(ms^2 + cs + k)X(s) = Z(s) \tag{3.2}$$

$$\frac{X(s)}{Z(s)} = \frac{1}{ms^2 + cs + k} \tag{3.3}$$

In Equation (3.2) and (3.3), Z(s) and X(s) are the input and output, respectively. The input, output and transfer function of the system are consisted of the dynamic model of the system. This model is illustrated as a block diagram:

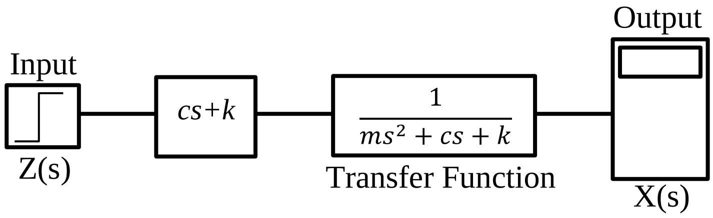

Figure 3.2 Block diagram for a damped system

In figure 3.2, the step input is applied to the transfer function of the system and obtained a vibration response. This unshaped response exists residual vibration. If the posicast control method is applied to the system, the residual vibration is eliminated. The half-cycle posicast and the three-step cycle posicast form are given as block diagram in Figure 3.3:

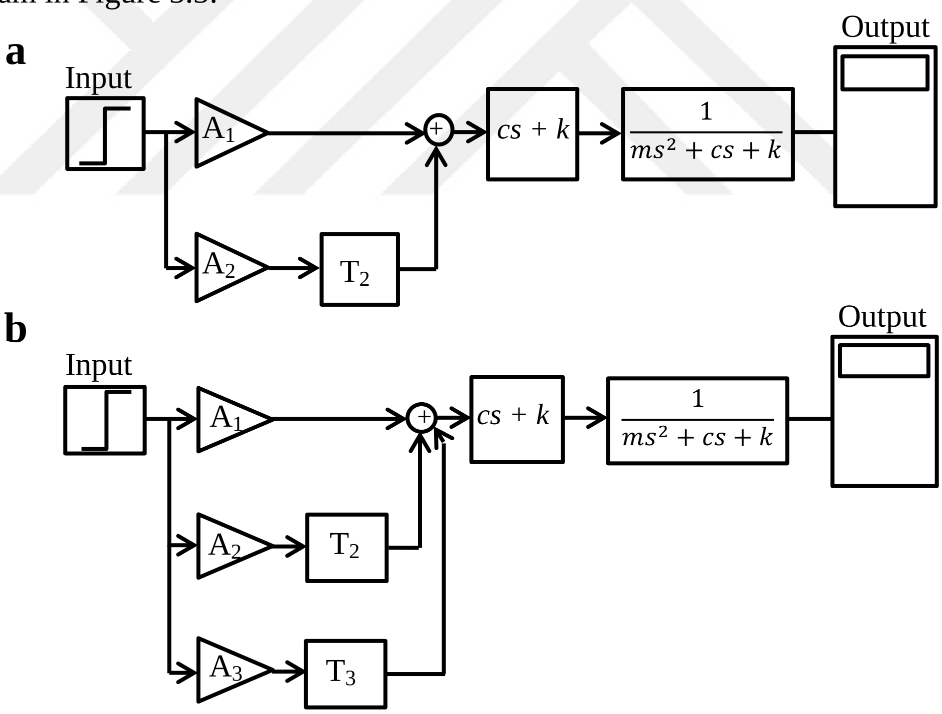

Figure 3.3 The block diagram of the posicast control (**a** half-cycle posicast, **b** three-step cycle posicast)

The posicast control method is determined as feedforward posicast design. The half-cycle posicast is shown in Figure 3.3(**a**) and the three-step cycle posicast form is given in Figure 3.3(**b**). The mass-spring-damper system parameters have been determined according to a sample of the planar manipulator which used previous studies (Malgaca, Yavuz, Akdağ & Karagülle, 2016). Total weight of the payload, sensor and manipulator are determined as mass of the S-DOF system. Damping constant is found through relation of critical damping and damping ratio as given in Equation (3.4-**a**). Stiffness constant is found from Hooke's Law in Equation (3.4-**b**). E, I and L are modulus of elasticity, inertia of cross section and length of the manipulator. x_d, F and c_c are deflection of spring, external force and critical damping, respectively (m=1.99 kg., c=0.9158 N.s/m. and k=1707.2 N/m.). Posicast amplitudes and delay times are computed in respect to Section 2 and given in Table 3.1:

$$\textbf{a} \quad c = \zeta \, . \, c_c \qquad \textbf{b} \quad F = k \, . \, x_d \qquad \textbf{c} \quad k = \frac{3 \, . \, E \, . \, I}{L^3} \tag{3.4}$$

Table 3.1 The parameters of the posicast control for the single-degree-of-freedom system

Cycles	A_1	A_2	A_3	T_2	T_3
One	0.2563	0.4999	0.2439	0.1080	0.2160
Half	0.5062	0.4938	-	0.1080	-
One-third	0.9958	-0.9752	0.9794	0.0360	0.0720
One-quarter	1.6955	-2.3700	1.6745	0.0270	0.0540
One-fifth	2.5963	-4.1669	2.5706	0.0216	0.0432
One-sixth	3.6975	-6.3644	3.6670	0.0180	0.0360
One-seventh	4.9988	-8.9621	4.9634	0.0154	0.0309

The unshaped system Figure 3.2 and the shaped system with the half-cycle posicast are given in Figure 3.4(**a**). The unshaped system is compared to the three-step cycle form in Figure 3.4(**b**). The reference input is the step input. We obtain:

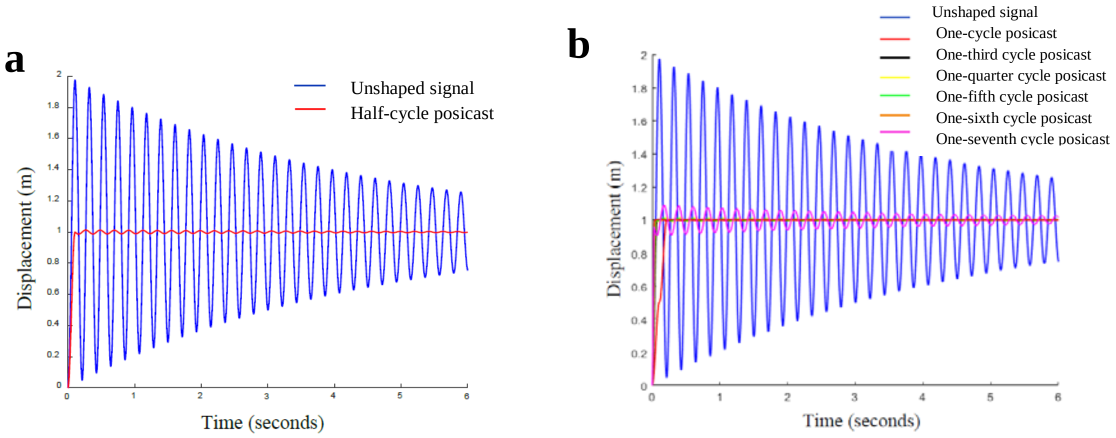

Figure 3.4 Comparison of the unshaped signal with the half-cycle (**a**), the three-step cycles (**b**)

3.2 The Multi-Degree-Of-Freedom System

In this section, M-DOF spring-mass-damper system as shown in Figure 3.5 is studied using the posicast method (Yavuz, Malgaca and Karagülle, 2016):

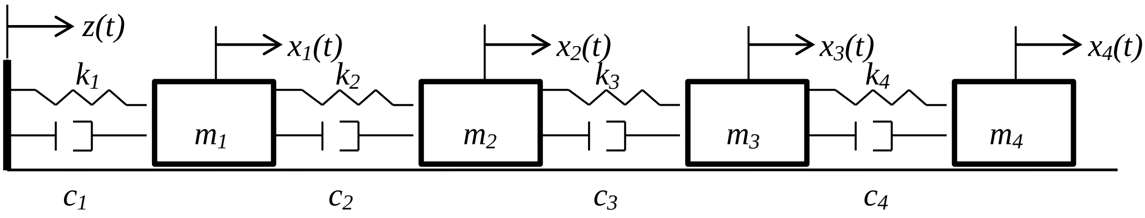

Figure 3.5 The mathematical model of the four-degree-of-freedom system

In Equation (3.2), the equation of motion is given in matrix form as shown below:

$$[m]\ddot{x} + [c]\dot{x} + [k]x = \mathrm{z(t)} \tag{3.5}$$

When the mass, spring and damping constants are arranged, the matrices of the four-degree-of-freedom system:

$$m = \begin{bmatrix} m_1 & 0 & 0 & 0 \\ 0 & m_2 & 0 & 0 \\ 0 & 0 & m_3 & 0 \\ 0 & 0 & 0 & m_4 \end{bmatrix} \quad c = \begin{bmatrix} c_1 + c_2 & -c_2 & 0 & 0 \\ -c_2 & c_2 + c_3 & -c_3 & 0 \\ 0 & -c_3 & c_3 + c_4 & -c_4 \\ 0 & 0 & -c_4 & c_4 \end{bmatrix}$$

$$k = \begin{bmatrix} k_1 + k_2 & -k_2 & 0 & 0 \\ -k_2 & k_2 + k_3 & -k_3 & 0 \\ 0 & -k_3 & k_3 + k_4 & -k_4 \\ 0 & 0 & -k_4 & k_4 \end{bmatrix}$$

The four-degree-of-freedom system has four displacements because of number of the masses. If the equation converts by Laplace transform, the output of the system is X_4(s) and the input is Z_1(s). Thus, the transfer function of the system is determined from H_{4n} row with respect to X_4(s). If the input force is Z_1(s), the matrix form is given based on Equation (3.3):

$$\begin{Bmatrix} X_1(s) \\ X_2(s) \\ X_3(s) \\ X_4(s) \end{Bmatrix} = \begin{bmatrix} H_{11} & H_{12} & H_{13} & H_{14} \\ H_{21} & H_{22} & H_{23} & H_{24} \\ H_{31} & H_{32} & H_{33} & H_{34} \\ H_{41} & H_{42} & H_{43} & H_{44} \end{bmatrix} \begin{Bmatrix} Z_1(s) \\ 0 \\ 0 \\ 0 \end{Bmatrix}$$

$$X_4(s) = Z_1(s)H_{41}(s) + Z_2(s)H_{42}(s) + Z_3(s)H_{43}(s) + Z_4(s)H_{44}(s) \quad (3.6)$$

In Equation (3.6), $H_{41}(s)$ is multiplied by the input $Z_1(s)$ with respect to the output $X_4(s)$. Thus, the transfer function of the system is $H_{41}(s)$ for the open-loop system.

The amplitudes and the delay times of the posicast method is determined by obtaining basic parameters of the system as given in the previous section in Equations (2.14), (2.23), (2.24), (2.25). The parameters are found by eigenvalues of the system. The eigenvalues are roots of the denominator of the transfer function. The denominator is:

$$as^n + bs^{n-1} + cs^{n-2} + \cdots + ds^0 = 0 \quad (3.7)$$

where a, b, c, d are coefficients and n is the order of the polynom. The roots consist of complex conjugate roots as x±yi. x and y are real and imaginary parts of the root. The parameters of the system is determined from the complex conjugate roots. The posicast method is applied into the open-loop transfer function H_{41}. This process is given as block diagram in Figure 3.6:

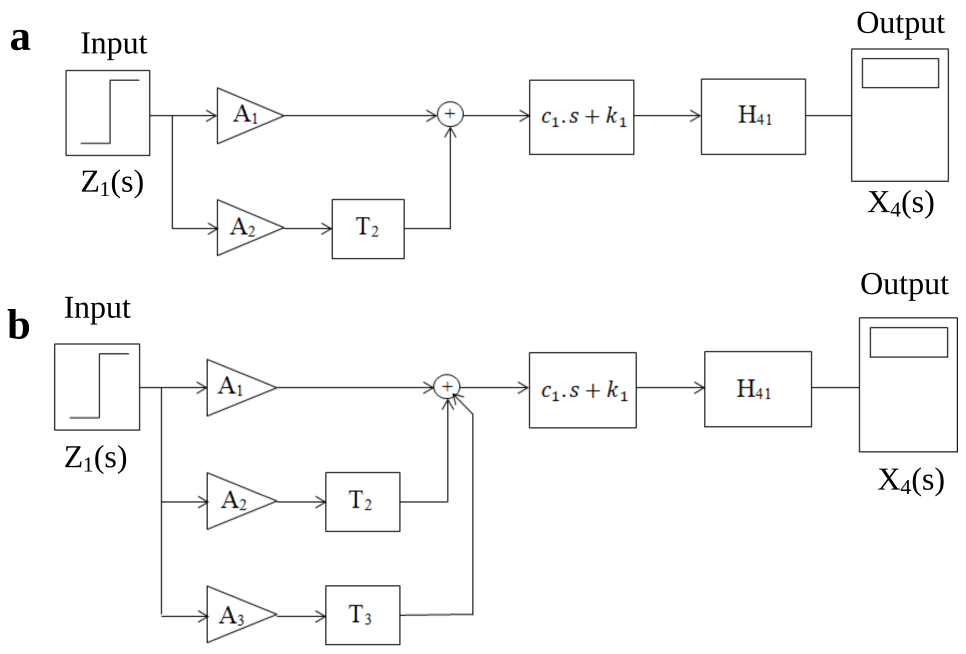

Figure 3.6 The block diagram form of the posicast control method (**a** half-cycle posicast, **b** three-step cycle posicast)

The numeric values of the four-degree-of-freedom system is given. The masses $m_1=m_2=m_3=m_4=1$ kg. The damping constants are $c_1=1.5$ Ns/m., $c_2=1.2$ Ns/m., $c_3=c_4=0.8$ Ns/m. The spring constants are $k_1=600$ N/m., $k_2=400$ N/m., $k_3=k_4=200$ N/m. If the open-loop transfer function H_{41} is defined as:

$$H_{41}(s) = \frac{192s^3 + 160{,}000s^2 + 44{,}000{,}000s + 4{,}000{,}000{,}000}{D_{41}(s)} \tag{3.8}$$

$$\begin{aligned} D_{41}(s) = {} & 250s^8 + 1775s^7 + 553{,}810s^6 + 2.333x10^6s^5 + 3.524x10^8s^4 \\ & + 7.074x10^8s^3 + 7.016x10^{10}s^2 + 3.24x10^{10}s + 2.4x10^{12} \end{aligned} \tag{3.9}$$

The numeric values of the four-degree-of-freedom system is given in Table 3.2:

Table 3.2 The parameters of the posicast control for the four-degree-of-freedom system

Cycles	**A_1**	**A_2**	**A_3**	**T_2**	**T_3**
One	0.2588	0.4998	0.2414	0.4799	0.9597
Half	0.5223	0.4777	-	0.4799	-
One-third	1.0115	-0.9999	0.9883	0.1600	0.3199
One-quarter	1.7218	-2.4139	1.6921	0.1200	0.2399
One-fifth	2.6360	-4.2355	2.5995	0.0960	0.1919
One-sixth	3.7533	-6.4633	3.7100	0.0800	0.1600
One-seventh	5.0735	-9.0967	5.0232	0.0686	0.1371

The posicast control method is applied to the system as given in Figure 3.6:

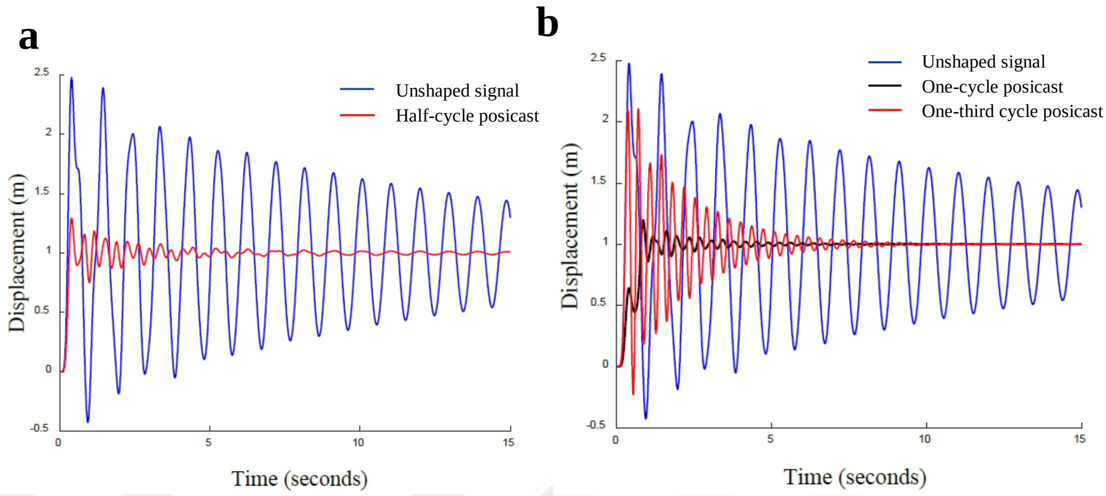

Figure 3.7 Comparison of the unshaped signal with the half-cycle (**a**), the three-step cycles (**b**)

The unshaped signal and the posicast controlled signals are compared in Figure 3.7. The half-cycle posicast and the three-step cycle posicast form are given in Figure 3.7(**a**) and Figure 3.7(**b**), respectively.

3.3 The Flexible Single-Link Planar Manipulator System

The examined system is called the single-link flexible planar manipulator (Malgaca, Yavuz, Akdağ and Karagülle, 2016). The initial point O is fixed and connected to a motor shaft. The end-point is free.

The manipulator is consisted of a beam. A revolute joint is located between O and the beam. A servomotor is applied to activate the beam. The flexible mechanism has been exposed to a payload. Furthermore, a sensor is employed to compute the accelerations. The sensor is considered as the second mass in this thesis. In this study, vibration magnitudes are evaluated by performing the input shaper compared to the unshaped reference inputs.

The planar manipulator is given as a perspective in Figure 3.8 (Malgaca, Yavuz, Akdağ and Karagülle, 2016):

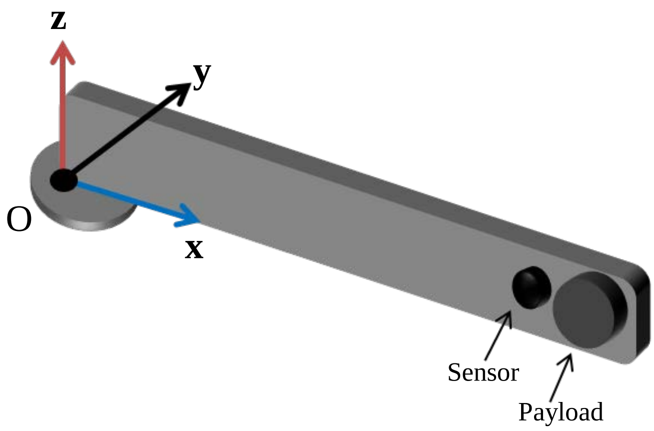

Figure 3.8 Flexible planar manipulator

The system has two masses that are the sensor at the background and the payload at the foreground. The single-link flexible manipulator is modelled by ANSYS as shown in Figure 3.9 and given dimensions in Figure 3.10:

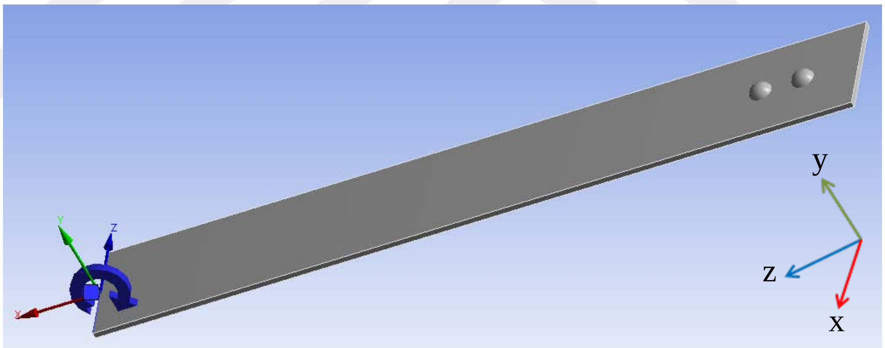

Figure 3.9 ANSYS model

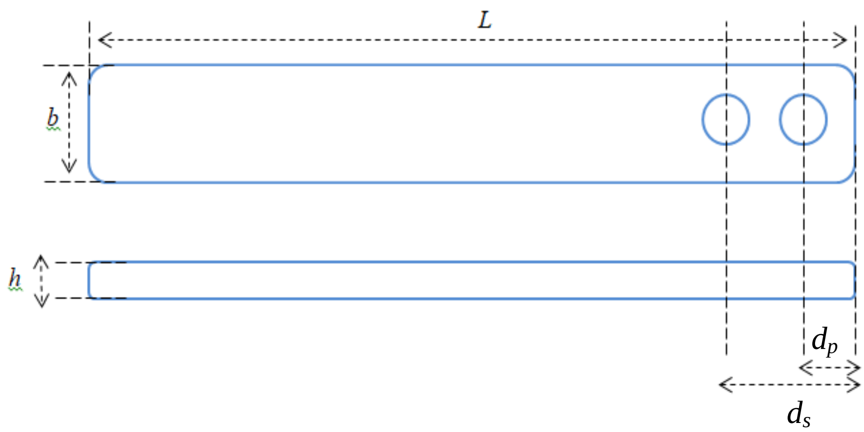

Figure 3.10 Dimensions of the flexible planar manipulator

Table 3.3 The numeric values of the flexible planar manipulator

Modulus of elasticity, *E*	210 GPa
Density, ρ	7850 kg/m^3
Length, *L*	540 mm
Distance of the payload from the end-point *d* payload	40 mm
Distance of receiving point from the end-point *d* sensor	70 mm
Thickness, *h*	4 mm
Width, *b*	80 mm
Cross section area, *A*	320 mm^2
Inertia of cross section, *I*	426.67 mm^4
Number of finite elements, *n*e	2256
Rayleigh damping coefficient, *B*	4×10^{-4}
Weight of the sensor, m_s	0.054 kg
Weight of the payload, m_L	0.62 kg
Motor rotational spring constants, K_m	16000 N.m/rad

In the Table 3.3, the numeric values are illustrated as parameters of the flexible planar manipulator. There is joint flexibility in the servo motor. Thus, the motor has a spring constant K_m as rotational. d_p and d_s are distance of the payload and sensor in Figure 3.10, respectively. The manipulator has 2256 elements as the finite element FE.

The lumped-parameter systems and the single-link flexible manipulator are given as numerical and graphical results. Then, evaluating of the results are written. Trapezoidal motion input is applied to over-all the systems as the reference input. This unshaped input is exposed to the posicast control input.

The amplitudes and the delay times of the posicast method are given as the numeric values in Table 3.4:

Table 3.4 The numeric values of the posicast method for the flexible planar manipulator system

Cycles	A_1	A_2	A_3	T_2	T_3
One	0.2518	0.5000	0.2482	0.0692	0.1384
Half	0.5065	0.4935	-	0.0692	-
One-third	1.0024	-1.0000	0.9976	0.0231	0.0461
One-quarter	1.7102	-2.4142	1.7040	0.0173	0.0346
One-fifth	2.6219	-4.2360	2.6142	0.0138	0.0277
One-sixth	3.7366	-6.4641	3.7275	0.0115	0.0231
One-seventh	5.0542	-9.0978	5.0436	0.0099	0.0198

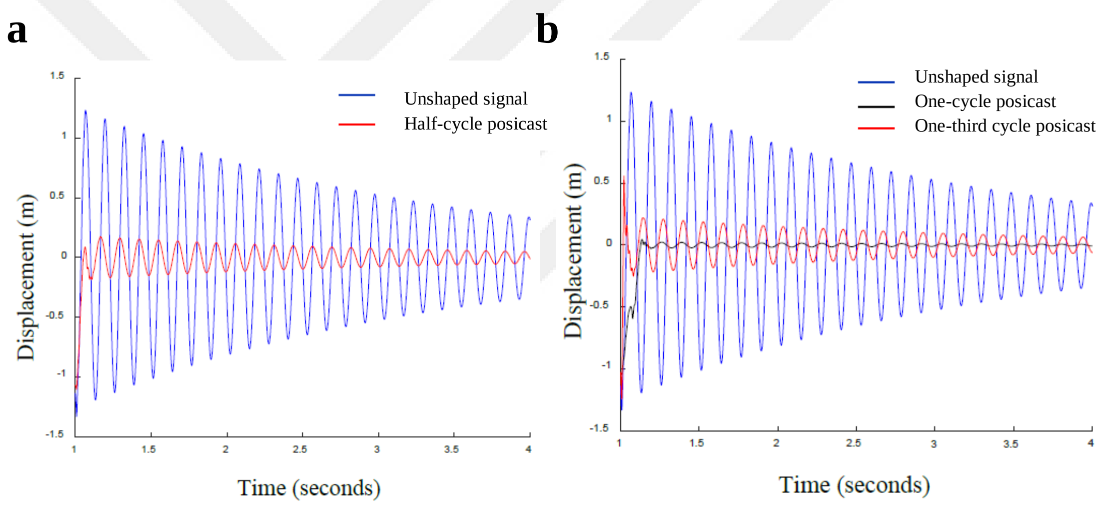

Figure 3.11 Comparison of the unshaped signal with the half-cycle (**a**), the three-step cycles (**b**)

The unshaped and the posicast controlled signals are shown in Figure 3.11. The unshaped signal is compared to the half-cycle posicast in Figure 3.11(**a**) and the three-step cycles in Figure 3.11(**b**).

3.4 Motion Profile

Generalized trapezoidal motion graph (**a**) and angular trajectory of a manipulator (**b**) are given as Figure 3.12:

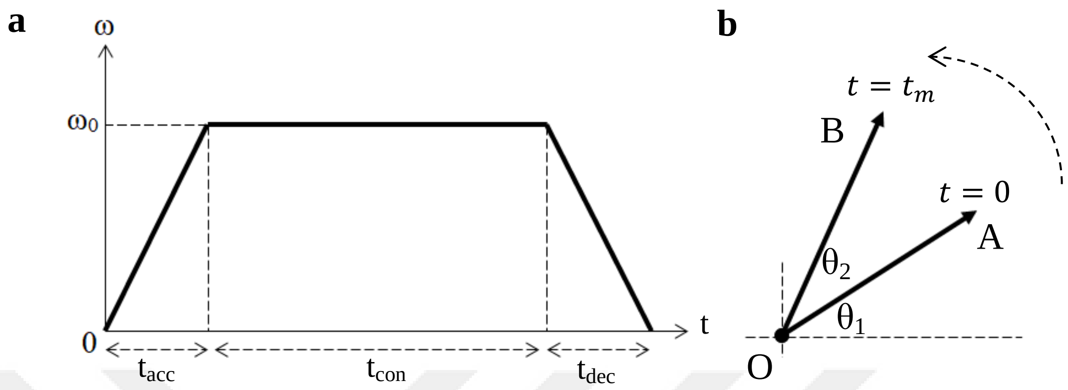

Figure 3.12 Generalized trapezoidal motion graph (**a**), angular motion of the manipulator (**b**)

The posicast method is dealt with the step input. The method is also adapted for the trapezoidal profile. The trapezoidal input is given in Figure 3.12(**a**). In addition, the motion of a manipulator is demonstrated under effect of the trapezoidal profile in Figure 3.12(**b**). t_{acc}, t_{con} and t_{dec} are accelerated motion, constant velocity motion and decelerated motion in time t. ω_0 and t_m are maximum angular velocity and motion time, respectively.

Initial angular position starts OA in t=0. Second angular position locates OB in $t=t_m$. First angular motion is θ_1 in t=0. Second angular motion is $\theta_{12}=\theta_1+\theta_2$ in $t=t_m$. θ_2 corresponds to area under the velocity curve as given in Figure 3.12(**a**). The numeric values of the velocity and the time intervals of the trapezoidal motion profile as formula are based on the reference article (Malgaca, Yavuz, Akdağ and Karagülle, 2016).

The computed numeric values of the trapezoidal motion profile is given in Table 3.5:

Table 3.5 The numeric values of the trapezoidal motion profile

TM-1	$\boldsymbol{\omega_0}$	$\mathbf{t_{acc}}$	$\mathbf{t_{con}}$	$\mathbf{t_{dec}}$
30°	0.8727	0.4	0.2	0.4
60°	1.7453	0.4	0.2	0.4

TM-2	$\boldsymbol{\omega_0}$	$\mathbf{t_{acc}}$	$\mathbf{t_{con}}$	$\mathbf{t_{dec}}$
30°	0.3272	0.4	1.2	0.4
60°	0.6545	0.4	1.2	0.4

Note that, TM-1 and TM-2 are the first and the second motion times, respectively. TM-1 equals to 1 s. and TM-2 equals to 2 s. The trapezoidal motion profile is realized 30° and 60° capability of the motions.

CHAPTER FOUR

RESULTS AND DISCUSSIONS

In this section, the posicast method is applied to the single-degree-of-freedom system, the multi-degree-of-freedom system and the flexible planar manipulator as given in Section 3. The posicast cycles are performed as the half-cycle, the one-cycle, the one-third cycle, the one-quarter cycle, the one-fifth cycle, the one-sixth cycle and the one-seventh cycle, respectively. Only the unshaped signal, the half-cycle, the one-cycle and the one-seventh cycle are employed in graphical results. The entire results are indicated as numeric values in Tables. The reference input is considered as a trapezoidal motion profile as given in Section 3.4. The single and the multi-degree-of-freedom systems are investigated in two velocity values as given in Table 3.5. The flexible planar manipulator is moved with two angular motion. The results are simulated as graphical form. Root mean square RMS and settling time values are given as tables (Kuo and Golnaraghi, 2017). RMS correspons to energy level of a vibration as given in Equation (4.1). Settling time is determined by staying at 0.2 percent of steady-state value within the vibration signals for the M-DOF system and the manipulator in this study. For the S-DOF system, settling time is determined 0.1 percent.

$$V = \sqrt{\frac{1}{T}\int_0^T V(t)^2 \, dt} \tag{4.1}$$

In Equation (4.1), V defines to generalized waveform. Period expression is T and t is the total time of the vibration response. The values of amplitude and delay time of the posicast method are indicated in Section 3 for the each system.

As indicated in Table 3.5, V_{max1} and V_{max2} are maximum velocities according to 30° and 60° angular motions of the manipulator, respectively.

4.1 Simulations Of The Single-Degree-Of-Freedom System

In this section, the unshaped input signals and vibration responses are simulated for the S-DOF system. On the other hand, shaped input signals and vibration responses are compared to the unshaped simulations. Figures 4.1(**a**), 4.1(**b**), 4.1(**c**) and 4.1(**d**) are input signals for V_{max1} in TM-1 and the unshaped, half-cycle, one-cycle and one-seventh cycle, respectively. Vibration responses are given for the unshaped and shaped input signals in Figure 4.2. The input signals of the unshaped and shaped system are given for V_{max2} in TM-1 in Figures 4.3(**a**), 4.3(**b**), 4.3(**c**) and 4.3(**d**). These graphs are expressed the unshaped, half-cycle, one-cycle and one-seventh cycle, respectively. Vibration response is simulated in Figure 4.4. For V_{max1} in TM-2, the input signals are simulated in Figure 4.5(**a**), 4.5(**b**), 4.5(**c**) and 4.5(**d**). The input signals have same sequence in terms of title of posicast cycles. Figure 4.6 is the vibration responses. For V_{max2} in TM-2, the input signals are given in Figures 4.7(**a**), 4.7(**b**), 4.7(**c**) and 4.7(**d**). The figures are the unshaped, half-cycle, one-cycle and one-seventh cycle, respectively. The vibration responses are given in Figure 4.8. The calculated dynamic parameters of the S-DOF system are calculated as ω_n=4.66 Hz., ω_d=4.66 Hz., damping ratio ζ=0.0079 and t_p=0.1080 s.

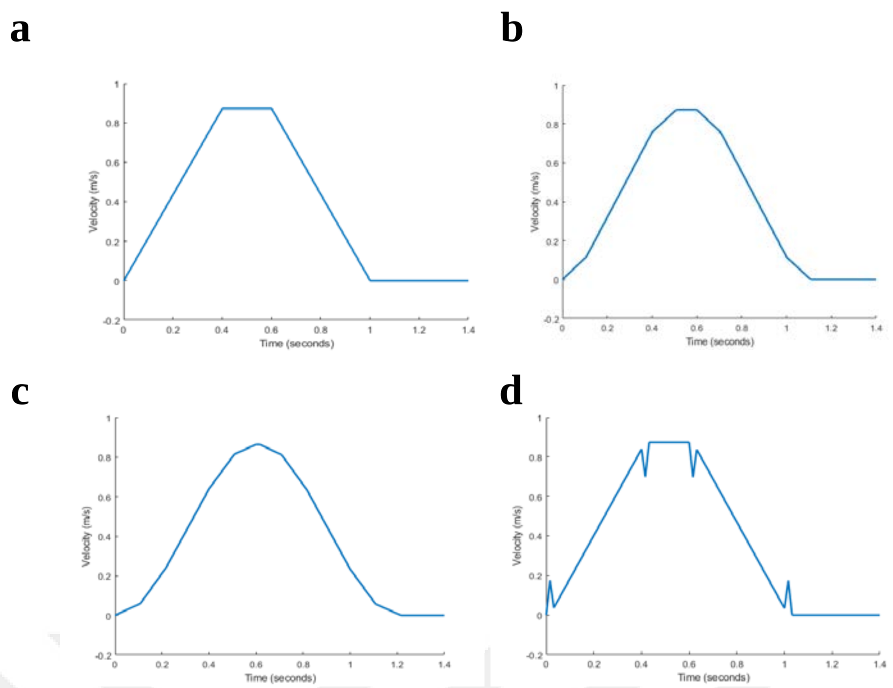

Figure 4.1 The input signals for V_{max1} in TM-1 (**a** unshaped, **b** half-cycle, **c** one-cycle, **d** one-seventh cycle)

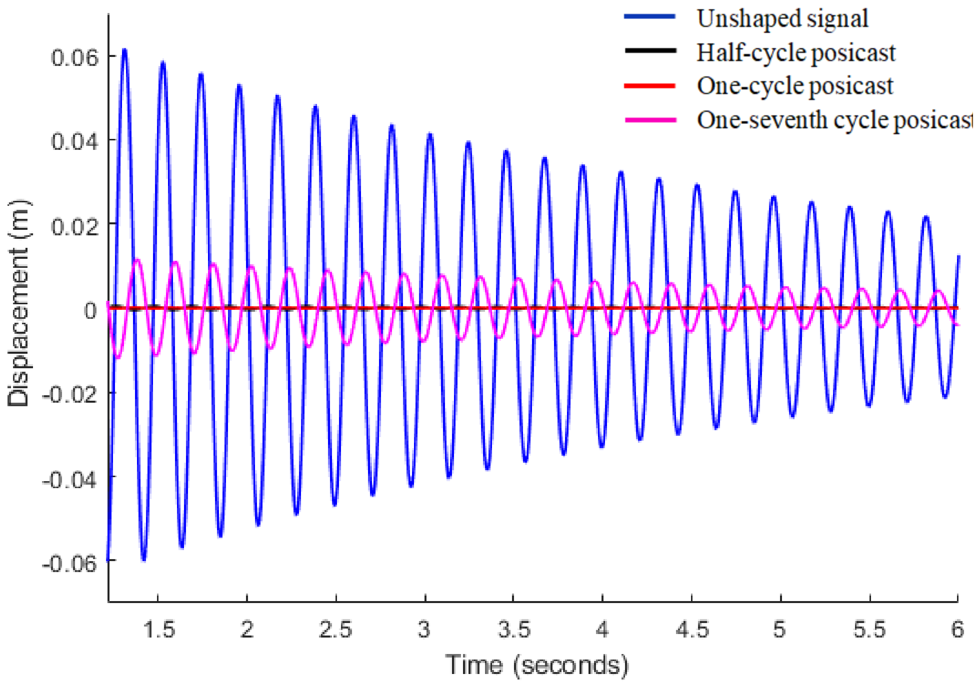

Figure 4.2 Comparison of the unshaped and the posicast controlled signals for V_{max1} in TM-1

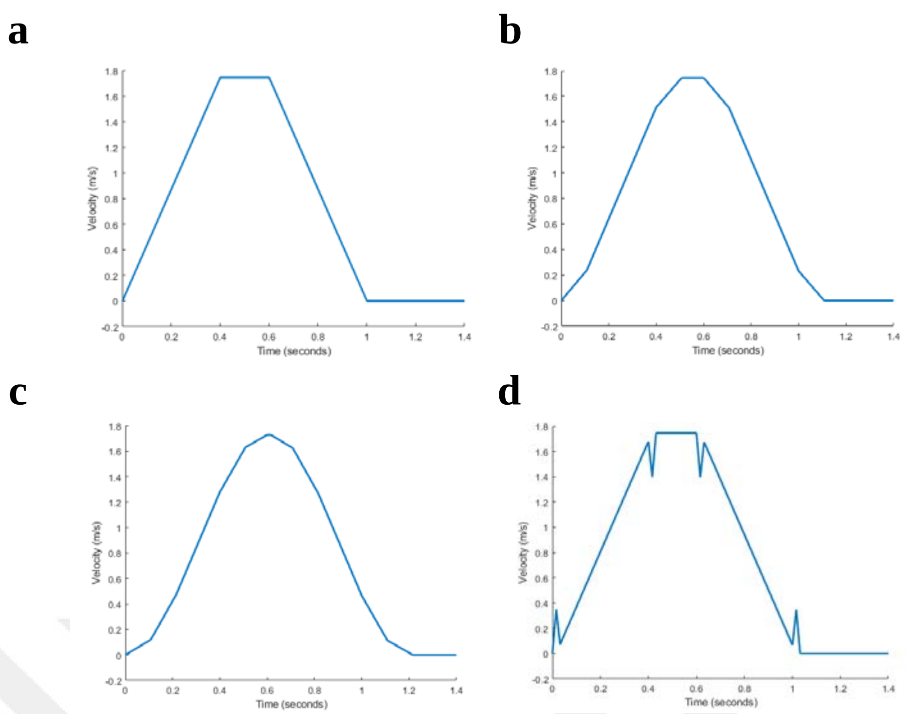

Figure 4.3 The input signals for V_{max2} in TM-1 (**a** unshaped, **b** half-cycle, **c** one-cycle, **d** one-seventh cycle)

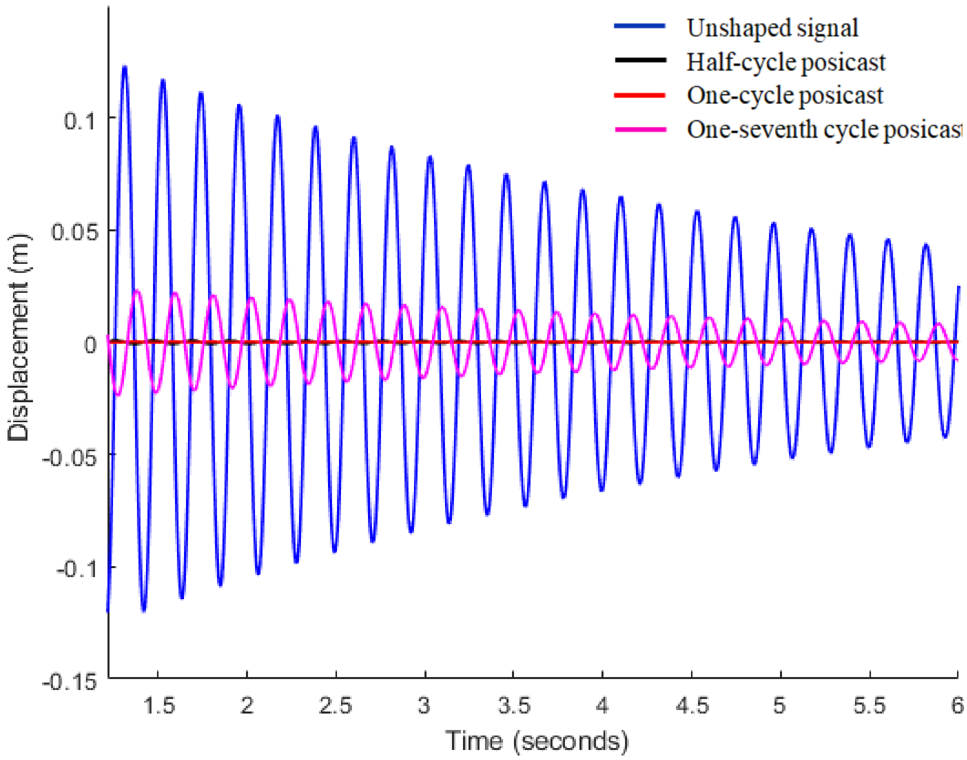

Figure 4.4 Comparison of the unshaped and the posicast controlled signals for V_{max2} in TM-1

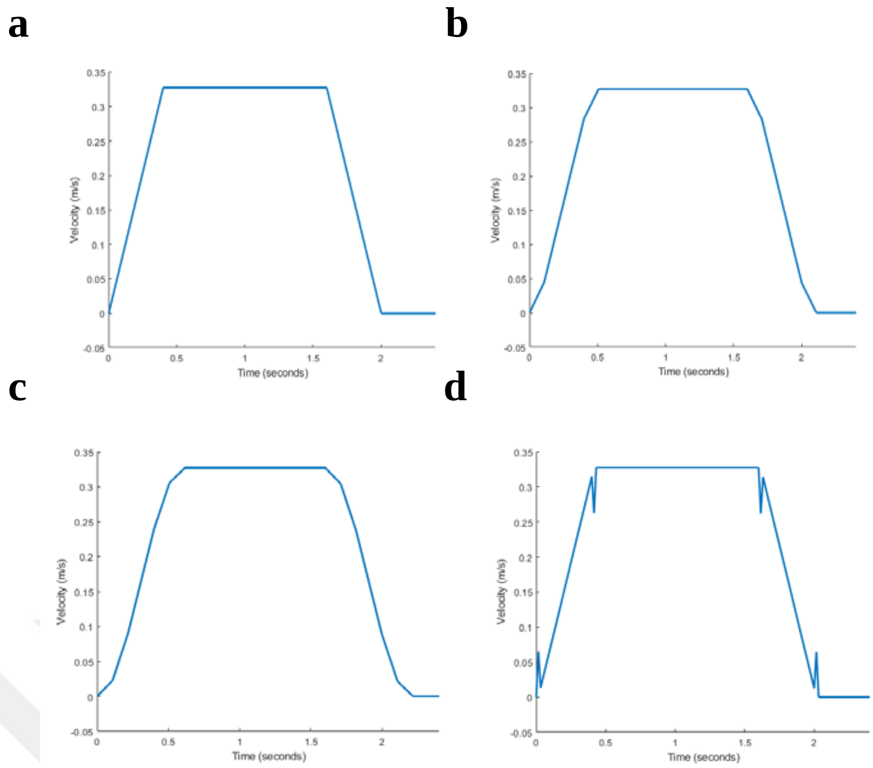

Figure 4.5 The input signals for V_{max1} in TM-2 (**a** unshaped, **b** half-cycle, **c** one-cycle, **d** one-seventh cycle)

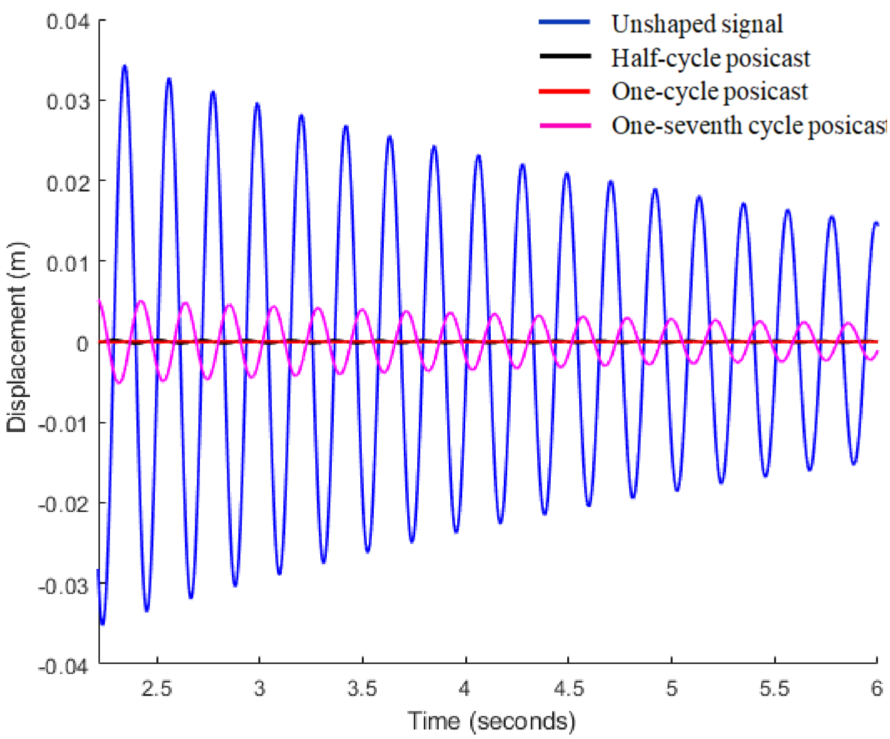

Figure 4.6 Comparison of the unshaped and the posicast controlled signals for V_{max1} in TM-2

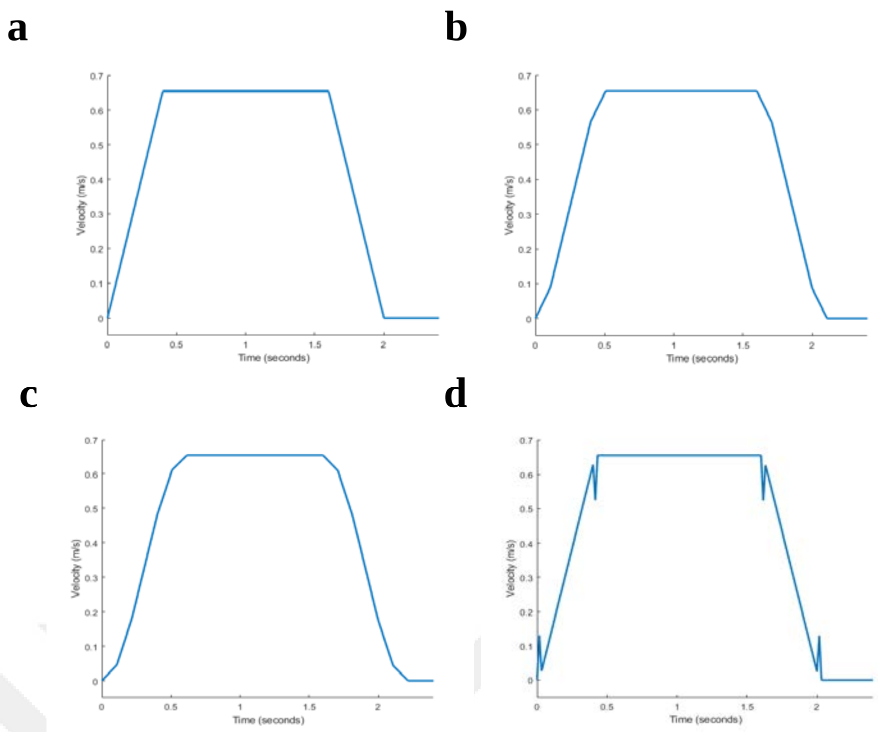

Figure 4.7 The input signals for V_{max2} in TM-2 (**a** unshaped, **b** half-cycle, **c** one-cycle, **d** one-seventh cycle)

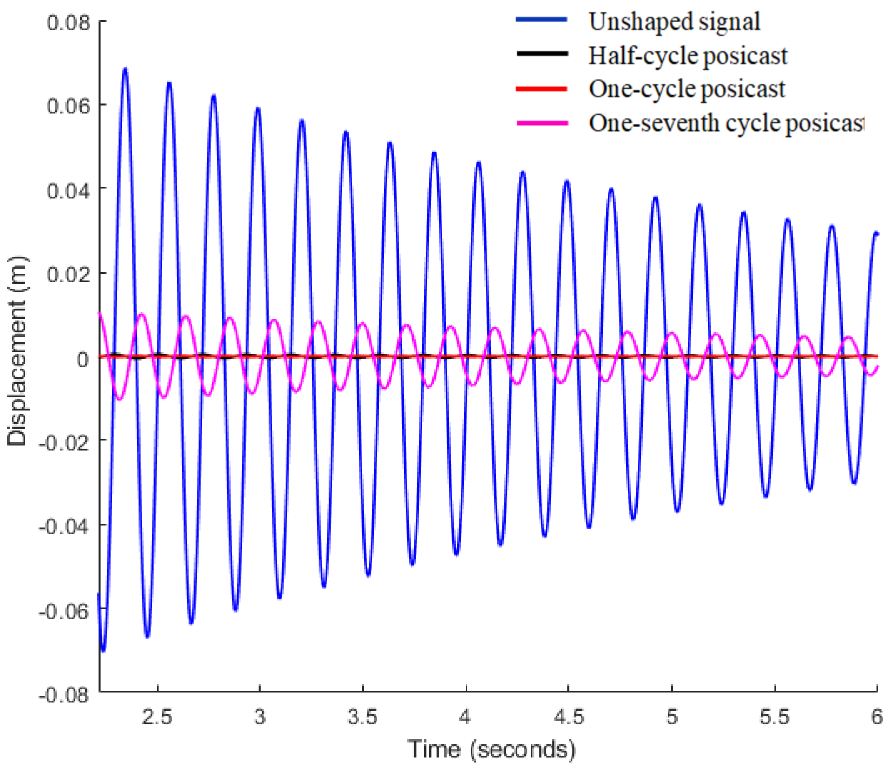

Figure 4.8 Comparison of the unshaped and the posicast controlled signals for V_{max2} in TM-2

The vibration responses are given in Figures 4.2, 4.4, 4.6 and 4.8. The unshaped, half-cycle, one-cycle and one-seventh cycle are simulated in these graphs. The entire results are illustrated as numeric values in Table 4.1 for S-DOF system. Table 4.1 indicates two maximum velocity as V_{max1} and V_{max2}. Also, RMS values of during motion and residual vibration cases as well as settling times values are given for the each velocity corresponding to the unshaped and shaped signals.

Table 4.1 Results of the S-DOF system

TM-1

	V_{max1}=0.8727 m/s			**V_{max2}=1.7453 m/s**		
Posicast Types (Cycles)	**During Motion RMS (m)**	**Residual Vibration RMS (m)**	**Settling Time (s)**	**During Motion RMS (m)**	**Residual Vibration RMS (m)**	**Settling Time (s)**
Unshaped	0.6078	0.0128	18.13	1.2156	0.0256	21.14
Half-Cycle	0.5647	8.84e-05	~0	1.1294	1.77e-04	~0
One-Cycle	0.5093	2.36e-05	~0	1.0186	4.71e-05	~0
One-third Cycle	0.5657	9.76e-05	~0	1.1315	1.95e-04	~0
One-quarter Cycle	0.5728	2.26e-04	0.681	1.1456	4.52e-04	3.686
One-fifth Cycle	0.5777	9.98e-04	7.102	1.1555	0.0020	10.11
One-sixth Cycle	0.5806	5.23e-04	4.301	1.1612	0.0010	7.309
One-seventh Cycle	0.5827	0.0024	10.97	1.1655	0.0049	13.98

TM-2

	V_{max1}=0.3272 m/s			**V_{max2}=0.6545 m/s**		
Posicast Types	**During Motion RMS (m)**	**Residual Vibration RMS (m)**	**Settling Time (s)**	**During Motion RMS (m)**	**Residual Vibration RMS (m)**	**Settling Time (s)**
Unshaped	0.2819	0.0074	15.68	0.5638	0.0147	18.69
Half-Cycle	0.2727	5.03e-05	~0	0.5454	1.01e-04	~0
One-Cycle	0.2586	1.34e-05	~0	0.5172	2.68e-05	~0
One-third Cycle	0.2729	5.36e-05	~0	0.5457	1.07e-04	~0
One-quarter Cycle	0.2746	1.25e-04	~0	0.5492	2.50e-04	1.935
One-fifth Cycle	0.2758	4.66e-04	4.711	0.5517	9.31e-04	7.716
One-sixth Cycle	0.2765	2.23e-04	1.489	0.5530	4.45e-04	4.483
One-seventh Cycle	0.2770	0.0011	8.372	0.5541	0.0022	11.38

As indicated in Table 4.1, values of RMS and the settling time are obtained by applying the trapezoidal inputs. The results are evaluated in terms of unshaped and shaped values.

In this study, the posicast control method is illustrated from one-cycle to one-seventh cycle posicast as the three-step cycle posicast. The one-cycle posicast is demonstrated superior damping quality compared to the other cycles for over-all cases. On the other hand, the one-seventh cycle is realized to the lowest damping quality.

As seen from Figure 4.2, the half-cycle posicast is carried out an efficient damping quality. RMS value decreases from 0.6078 to 0.5647 in during motion-RMS for V_{max1} for TM-1 as seen in Table 4.1. Furthermore, residual vibration-RMS decreases from 0.0128 to 8.84e-05. The half-cycle posicast is decreased the settling time to value of close to zero for V_{max1} in TM-1.

In Figure 4.4, this posicast method is mitigated from 1.2156 to 1.1294 RMS value for during motion-RMS for V_{max2} in TM-1. The half-cycle posicast is also decreased from 0.0256 to 1.77e-04 in residual vibration-RMS for V_{max2} in TM-1. The settling time is decreased to value of close to zero. As given in Figure 4.6, the posicast method is decreased RMS value from 0.2819 to 0.2727 during motion-RMS for V_{max1} in TM-2. In the same motion position, the S-DOF system has a mitigating from 0.0074 to 5.03e-05 in residual vibration-RMS. The half-cycle method is decreased the settling time to value of close to zero. In during motion-RMS, the value reduces from 0.5638 to 0.5454 for V_{max2} in TM-2 given as in Figure 4.8. The half-cycle posicast is decreased RMS value from 0.0147 to 1.01e-04 for residual vibration-RMS for V_{max2} in TM-2. The settling time equals to close to zero.

The three-step cycle posicast forms are illustrated in Table 4.1. The one-cycle posicast is realized reducing from 0.6078 to 0.5093 in during motion-RMS for V_{max1} in TM-1. On the other hand, the one-seventh cycle is illustrated poorly damping quality according to the other three-step cycle forms. Even if the one-seventh cycle is performed insufficient damping, the cycle is succeed reducing from 0.6078 to 0.5827. The one-cycle is decreased from 0.0128 to 2.36e-05 in residual vibration-RMS. The one-seventh cycle is shown reducing from 0.0128 to 0.0024 in residual vibration-RMS for V_{max1} in TM-1. For the settling time, the one-cycle posicast is accomplished eliminating the undesirable value. The one-seventh cycle is mitigated from 18.13 s. to 10.97 s. the settling time for V_{max1} in TM-1.

The one-cycle is reduced RMS value from 1.2156 to 1.0186 in during motion-RMS for V_{max2} in TM-1. In the same motion position, the one-seventh cycle is decreased RMS value from 1.2156 to 1.1655. In residual vibration-RMS for V_{max2} in TM-1, the one-cycle is realized mitigating RMS value from 0.0256 to 4.71e-05. The one-seventh cycle is reduced RMS value from 0.0256 to 0.0049. Although, the one-seventh cycle is the lowest damping quality, the cycle is created 80.9% damping rate. The one-cycle is decreased to the settling time in substantial level for V_{max2} in TM-1. The one-seventh cycle is decreased settling time from 21.14 s. to 13.98 s.

The one-cycle is carried out damping from 0.2819 to 0.2586 in during motion-RMS for V_{max1} in TM-2. The one-seventh cycle is reduced from 0.2819 to 0.2770. For residual vibration-RMS, the one-cycle is shown mitigating RMS value from 0.0074 to 1.34e-05 for V_{max1} in TM-2. The one-seventh cycle is decreased from 0.0074 to 0.0011 as RMS value. The one-cycle eliminates to the settling time in the same motion position, substantially. The one-seventh cycle is reduced from 15.68 s. to 8.372 s. that is corresponded to 46.61% damping rate.

In during motion-RMS for V_{max2} in TM-2, the one-cycle is realized diminishing from 0.5638 to 0.5172. On the other hand, the one-seventh cycle is decreased RMS value from 0.5638 to 0.5541. The one-cycle is carried out an efficient damping quality and mitigated RMS value from 0.0147 to 2.68e-05 in residual vibration-RMS for V_{max2} in TM-2. In this motion position, the one-seventh cycle is demonstrated the lowest damping performance. The cycle is reduced RMS value from 0.0147 to 0.0022. The one-cycle is accomplished eliminating the settling time for V_{max2} in TM-2, substantially. The one-seventh cycle is decreased from 18.69 s. to 11.38 s. the settling time.

4.2 Simulations Of The Multi-Degree-Of-Freedom System

The input shaping signals and its vibration responses are demonstrated for the M-DOF system. The input signals are simulated in Figures 4.9(**a**), 4.9(**b**), 4.9(**c**) and 4.9(**d**) for V_{max1} in TM-1. These simulations correspond to the unshaped, half-cycle, one-cycle and one-seventh cycle, respectively. The vibration responses of the inputs are given in Figure 4.10. For V_{max2} in TM-1, the input signals are illustrated in Figures 4.11(**a**), 4.11(**b**), 4.11(**c**) and 4.11(**d**). These graphs have the same configuration as sequence of the unshaped and shaped signals. Vibration responses are given in Figure 4.12. The other motion time TM-2 for V_{max1} is given in Figures 4.13(**a**), 4.13(**b**), 4.13(**c**) and 4.14(**d**) as the input signals. The vibration responses are illustrated in Figure 4.14. The input signals are demonstrated in Figure 4.15(**a**), 4.15(**b**), 4.15(**c**) and 4.15(**d**) for V_{max2} in TM-2. The vibration responses are given in Figure 4.16. For the M-DOF system, the dynamic characteristics are computed as ω_n=1.042 Hz., ω_d=1.041 Hz., damping ratio ζ=0.0111 and t_p=0.479 s.

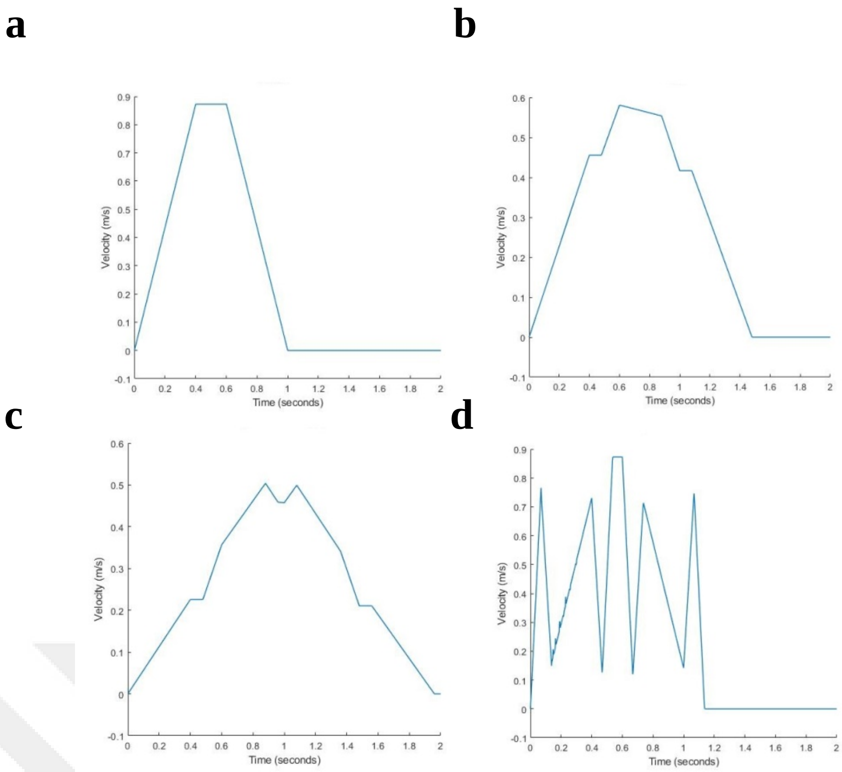

Figure 4.9 The input signals for V_{max1} in TM-1 (**a** unshaped, **b** half-cycle, **c** one-cycle, **d** one-seventh cycle)

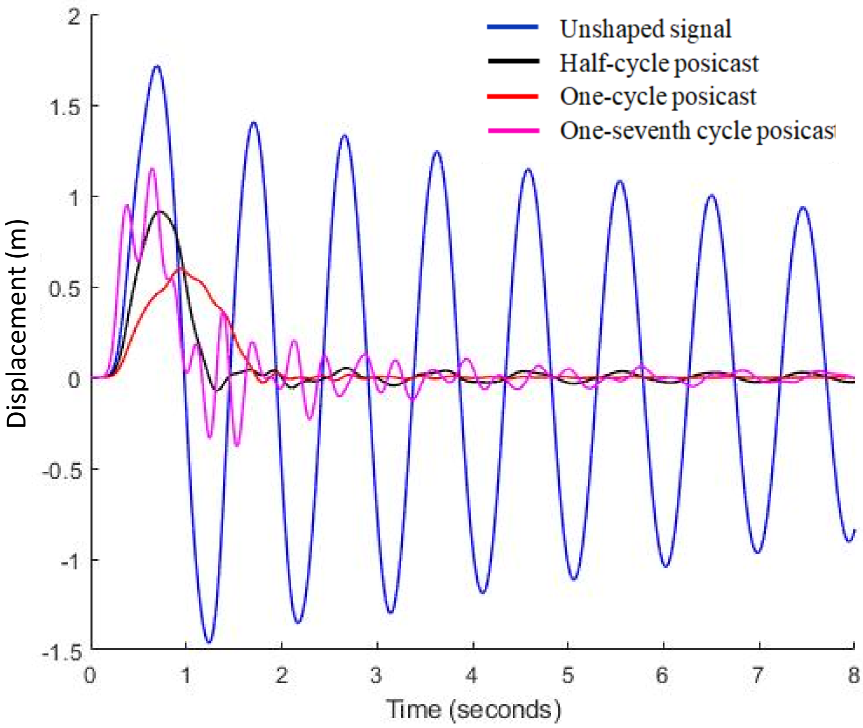

Figure 4.10 Comparison of the unshaped and the posicast controlled signals for V_{max1} in TM-1

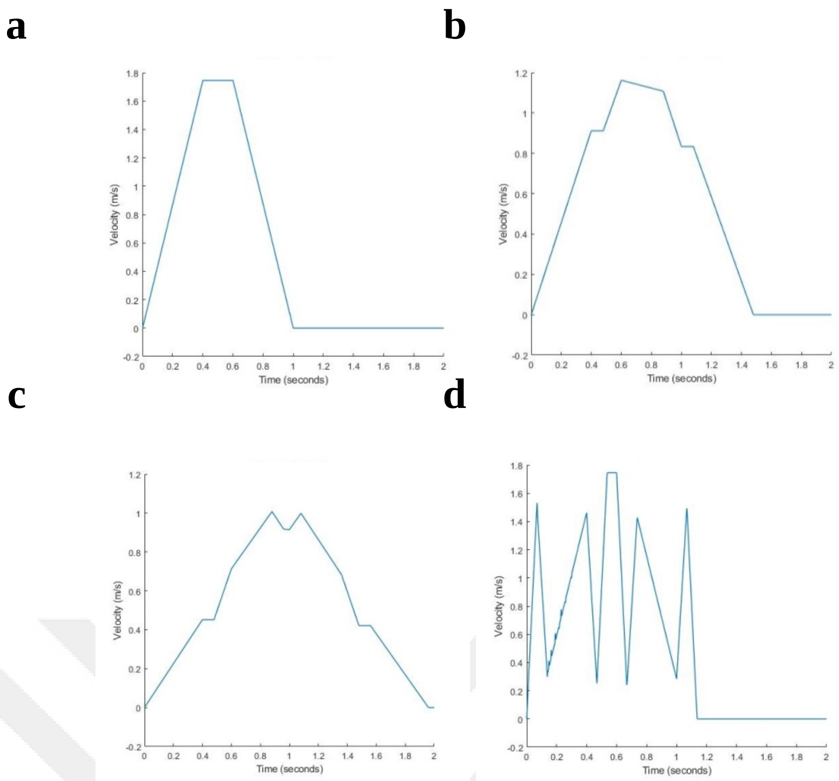

Figure 4.11 The input signals for V_{max2} in TM-1 (**a** unshaped, **b** half-cycle, **c** one-cycle, **d** one-seventh cycle)

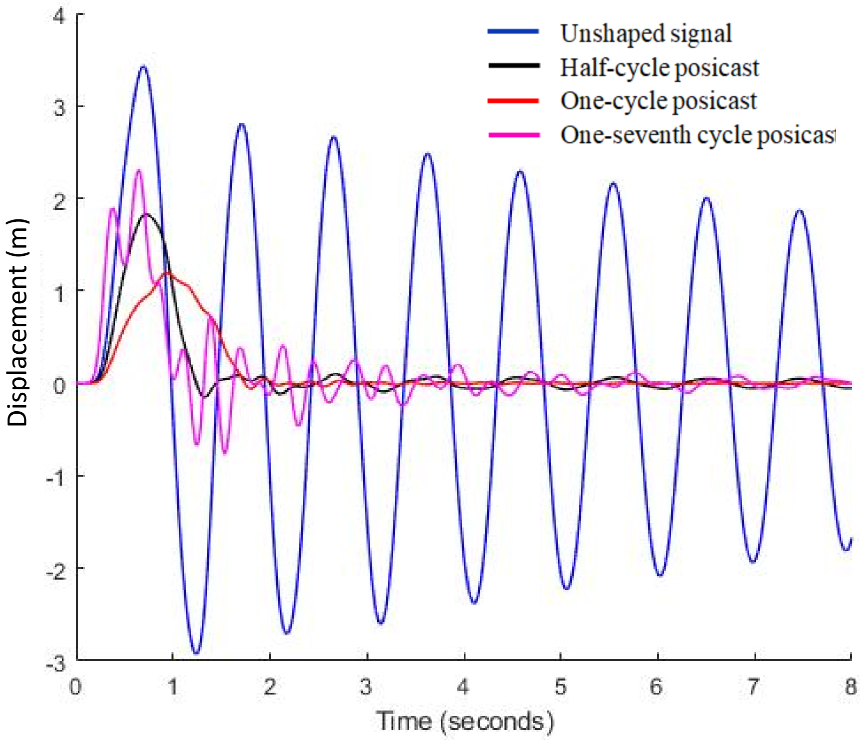

Figure 4.12 Comparison of the unshaped and the posicast controlled signals for V_{max2} in TM-1

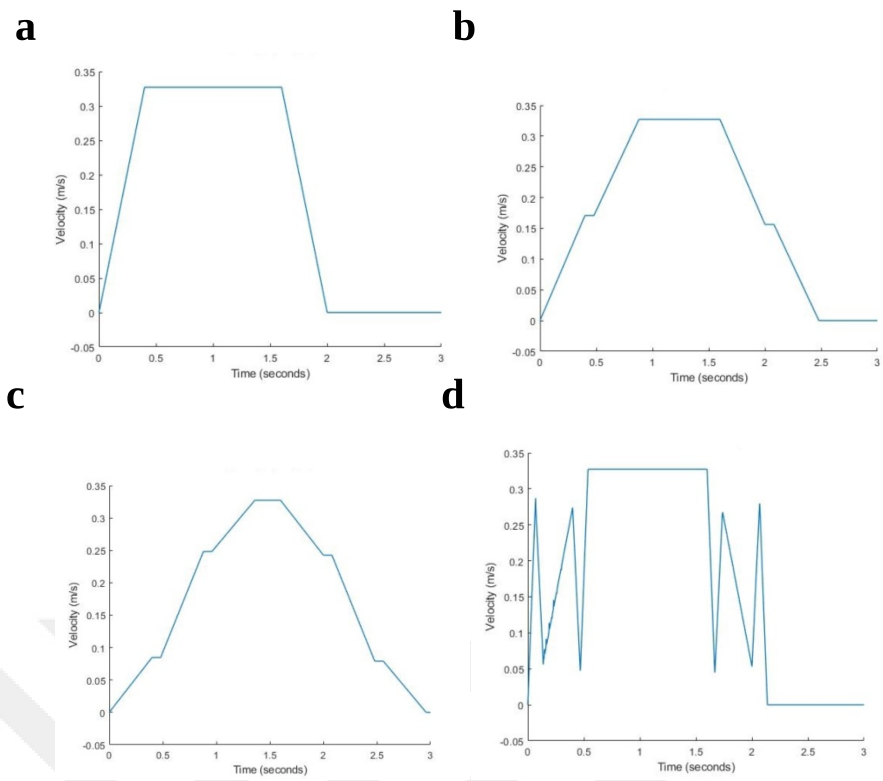

Figure 4.13 The input signals for V_{max1} in TM-2 (**a** unshaped, **b** half-cycle, **c** one-cycle, **d** one-seventh cycle)

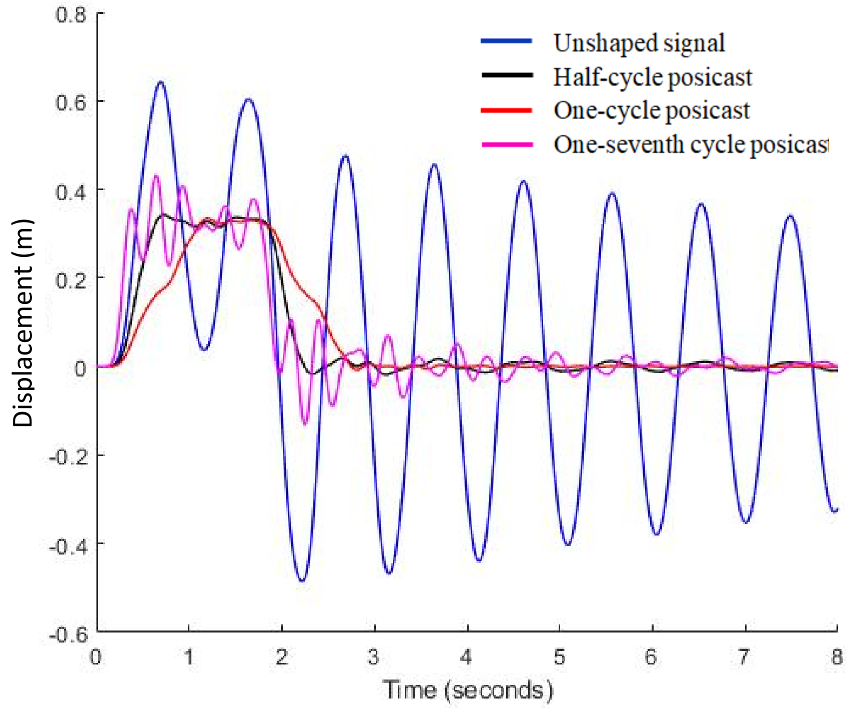

Figure 4.14 Comparison of the unshaped and the posicast controlled signals for V_{max1} in TM-2

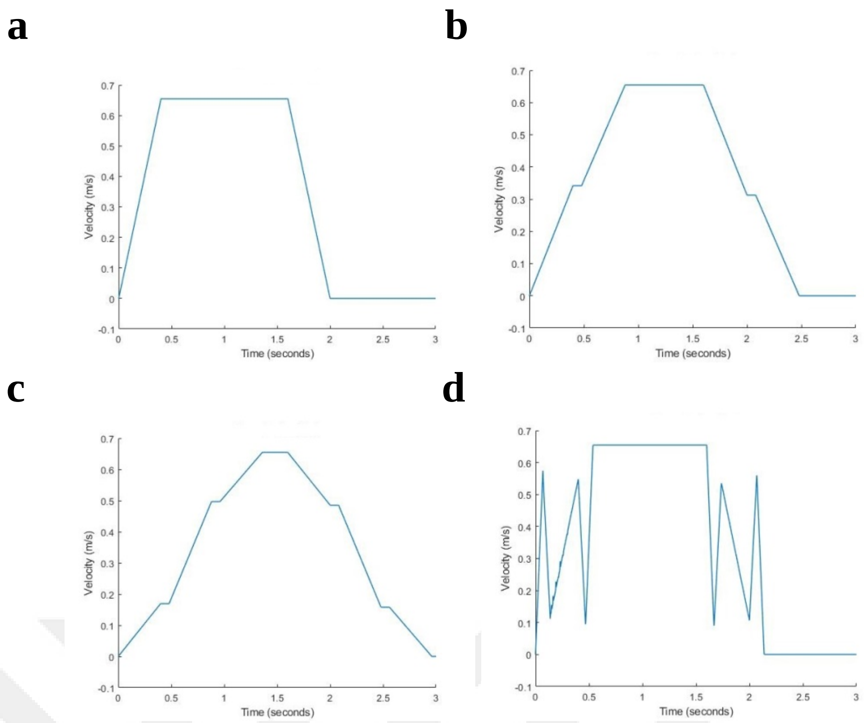

Figure 4.15 The input signals for V_{max2} in TM-2 (**a** unshaped, **b** half-cycle, **c** one-cycle, **d** one-seventh cycle)

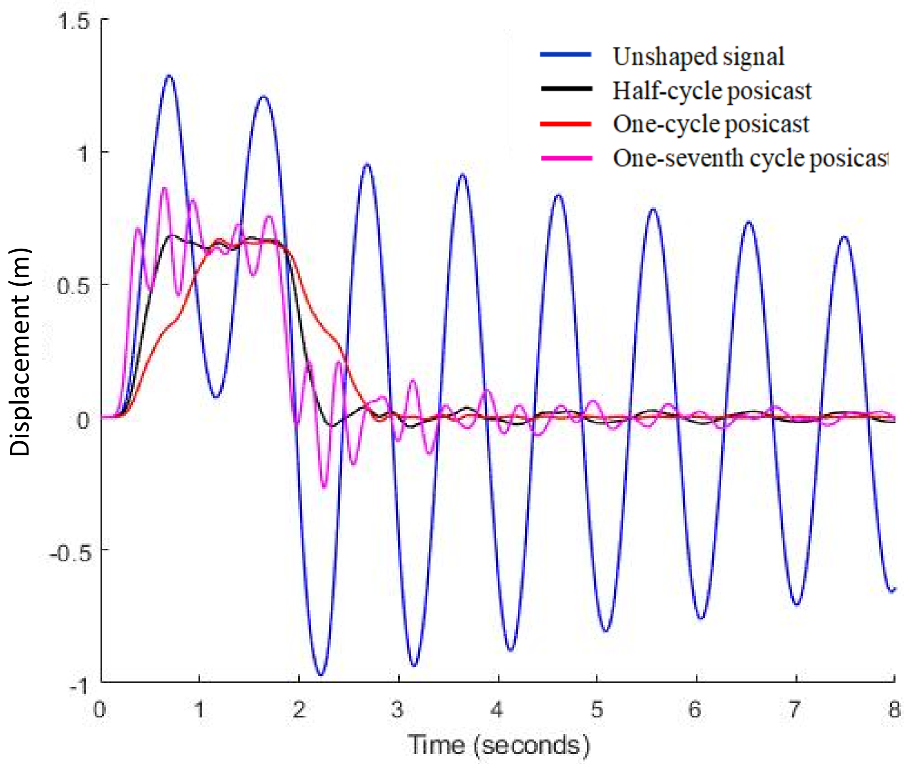

Figure 4.16 Comparison of the unshaped and the posicast controlled signals for V_{max2} in TM-2

As indicated in Table 4.2, all of the results of the unshaped and shaped signals are illustrated. During motion and residual vibration cases are given as RMS values. On the other hand, the settling time is demonstrated. The cases and the settling time are computed for the each velocity V_{max1} and V_{max2}. The maximum velocities are applied to the unshaped and shaped signals as given in Table 4.2:

Table 4.2 Results of the 4-DOF system

TM-1

	V_{max1}=0.8727 m/s			V_{max2}=1.7453 m/s		
Posicast Types	**During Motion RMS (m)**	**Residual Vibration RMS (m)**	**Settling Time (s)**	**During Motion RMS (m)**	**Residual Vibration RMS (m)**	**Settling Time (s)**
Unshaped	0.9893	0.2662	90.94	1.9786	0.5325	100.54
Half-Cycle	0.4989	0.0074	41.09	0.9979	0.0147	50.65
One-Cycle	0.3090	8.89e-04	5.337	0.6180	0.0018	10.56
One-third Cycle	0.5137	0.0087	21.29	1.0273	0.0174	30.86
One-quarter Cycle	0.5462	0.0139	28.62	1.0924	0.0279	38.19
One-fifth Cycle	0.5670	0.0174	34.84	1.1339	0.0348	43.98
One-sixth Cycle	0.5794	0.0203	39.68	1.1588	0.0405	49.26
One-seventh Cycle	0.5878	0.0224	44.01	1.1757	0.0449	53.59

TM-2

	V_{max1}=0.3272 m/s			V_{max2}=0.6545 m/s		
Posicast Types	**During Motion RMS (m)**	**Residual Vibration RMS (m)**	**Settling Time (s)**	**During Motion RMS (m)**	**Residual Vibration RMS (m)**	**Settling Time (s)**
Unshaped	0.3756	0.0909	76.03	0.7513	0.1818	85.68
Half-Cycle	0.2530	0.0025	26.19	0.5061	0.0050	35.80
One-Cycle	0.2008	2.78e-04	1.475	0.4016	5.56e-04	3.777
One-third Cycle	0.2562	0.0027	8.792	0.5125	0.0055	15.96
One-quarter Cycle	0.2653	0.0042	14.16	0.5307	0.0084	23.21
One-fifth Cycle	0.2710	0.0054	19.96	0.5419	0.0108	29.52
One-sixth Cycle	0.2745	0.0064	24.75	0.5490	0.0128	34.39
One-seventh Cycle	0.2770	0.0072	29.1	0.5540	0.0143	38.75

As seen in Table 4.2, the trapezoidal input is applied to the M-DOF system as given in Section 3. The half-cycle is realized an efficient damping quality in over-all cases. For three-step cycle posicast, the one-cycle is shown a superior damping quality. On the other hand, the one-seventh cycle is determined the lowest damping quality.

The half-cycle posicast is reduced RMS value from 0.9893 to 0.4989 in during motion-RMS for V_{max1} in TM-1. Residual vibration is reduced from 0.2662 to 0.0074 as RMS value. The half-cycle is decreased the settling time from 90.94 s. to 41.09 s. In during motion-RMS for V_{max2} in TM-1, RMS value is mitigated from 1.9786 to 0.9979. RMS value is diminished from 0.5325 to 0.0147 in residual vibration-RMS for V_{max2} in TM-1. The settling time is reduced from 100.54 s. to 50.65 s. The other motion position, the half-cycle posicast is decreased RMS value from 0.3756 to 0.2530 in during motion-RMS for V_{max1} in TM-2. The residual vibration-RMS is reduced from 0.0909 to 0.0025 for V_{max1} in TM-2. The settling time is diminished from 76.03 s. to 26.19 s. For V_{max2} in TM-2, RMS value is reduced from 0.7513 to 0.5061 during motion. The residual vibration is reduced from 0.1818 to 0.0050 as RMS value for V_{max2} in TM-2. The half-cycle posicast is decreased the settling time from 85.68 s. to 35.80 s.

The three-step cycles are compared to each other as the one-cycle and the one-seventh cycle. The one-cycle is accomplished damping quality at substantial level. On the other hand, the one-seventh cycle is realized the lowest damping quality compared to the other three-step cycles. The one-cycle is reduced RMS value from 0.9893 to 0.3090 in during motion-RMS for V_{max1} in TM-1. The one-seventh cycle is diminished RMS value from 0.9893 to 0.5878 in the same motion position. Residual vibration is decreased from 0.2662 to 8.89e-04 as RMS value for V_{max1} in TM-1 by the one-cycle posicast. The one-seventh cycle posicast is reduced RMS value from 0.2662 to 0.0224 in residual vibration-RMS for V_{max1} in TM-1. The settling time is reduced from 90.94 s. to 5.337 s. through the one-cycle posicast. The one-seventh cycle posicast is decreased from 90.94 s. to 44.01 s. to the settling time.

For V_{max2} in TM-1, RMS value is reduced from 1.9786 to 0.6180 during motion through the one-cycle posicast. The one-seventh cycle posicast is reduced RMS value from 1.9786 to 1.1757 in during motion-RMS for V_{max2} in TM-1. In the same motion position, the one-cycle posicast is decreased to residual vibration as RMS value from 0.5325 to 0.0018. The one-seventh cycle is realized mitigating damping from 0.5325 to 0.0449. The settling time is decreased from 100.54 s. to 10.56 s. through the one-cycle posicast. On the other hand, the one-seventh cycle posicast is diminished from 100.54 s. to 53.59 s. the settling time for V_{max2} in TM-1.

The one-cycle is diminished RMS value from 0.3756 to 0.2008 during motion for V_{max1} in TM-2. The one-seventh cycle is reduced from 0.3756 to 0.2770 in the same motion position. The one-cycle is decreased RMS value from 0.0909 to 2.78e-04 in residual vibration-RMS for V_{max1} in TM-2. The one-seventh cycle is decreased from 0.0909 to 0.0072. The settling time is reduced from 76.03 s. to 1.475 s. through the one-cycle for V_{max1} in TM-2. The one-seventh cycle is mitigated from 76.03 s. to 29.1 s. The one-cycle is realized diminishing ability to RMS value from 0.7513 to 0.4016 in during motion-RMS for V_{max2} in TM-2. On the other hand, the one-seventh cycle is reduced from 0.7513 to 0.5540. The one-cycle posicast is reduced RMS value from 0.1818 to 5.56e-04 in residual vibration-RMS for V_{max2} in TM-2. The one-seventh cycle is decreased from 0.1818 to 0.0143 in the same motion position. The settling time is mitigated from 85.68 s. to 3.777 s. through the one-cycle posicast. The one-seventh cycle is diminished the settling time from 85.68 s. to 38.75 s.

4.3 Simulations Of The Flexible Planar Manipulator System

The input signals are given in Figures 4.17(**a**), 4.17(**b**), 4.17(**c**) and 4.17(**d**) for TM-1 30°. The vibration responses are given in Figure 4.18. These graphs are the unshaped, half-cycle, one-cycle and one-seventh cycle, respectively. For TM-1 60°, the input signals are illustrated in Figure 4.19(**a**), 4.19(**b**), 4.19(**c**) and 4.19(**d**). The vibration responses of the input signals are demonstrated in Figure 4.20. The other motion position TM-2 30° is given in Figures 4.21(**a**), 4.21(**b**), 4.21(**c**) and 4.21(**d**) as the input signals. The vibration responses are illustrated in Figure 4.22 for the same motion position. The input signals are demonstrated in Figures 4.23(**a**), 4.23(**b**), 4.23(**c**) and 4.23(**d**) for TM-2 60°. The vibration responses are given in Figure 4.24. For the manipulator system, the dynamic parameters are computed as ω_n=7.223 Hz., ω_d=7.222 Hz., damping ratio ζ=0.0023 and t_p=0.0692 s.

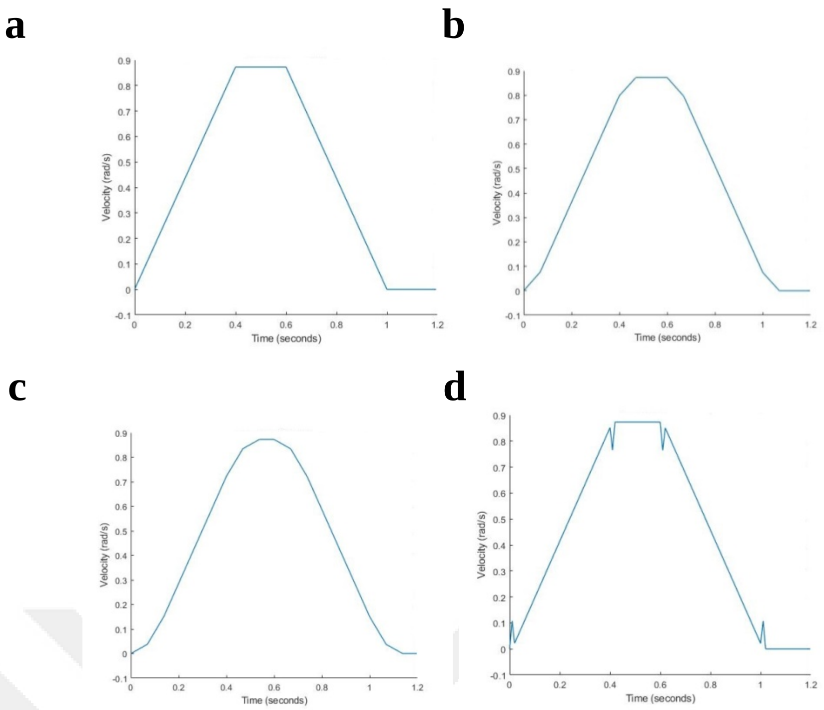

Figure 4.17 The input signals for TM-1 30° (**a** unshaped, **b** half-cycle, **c** one-cycle, **d** one-seventh cycle)

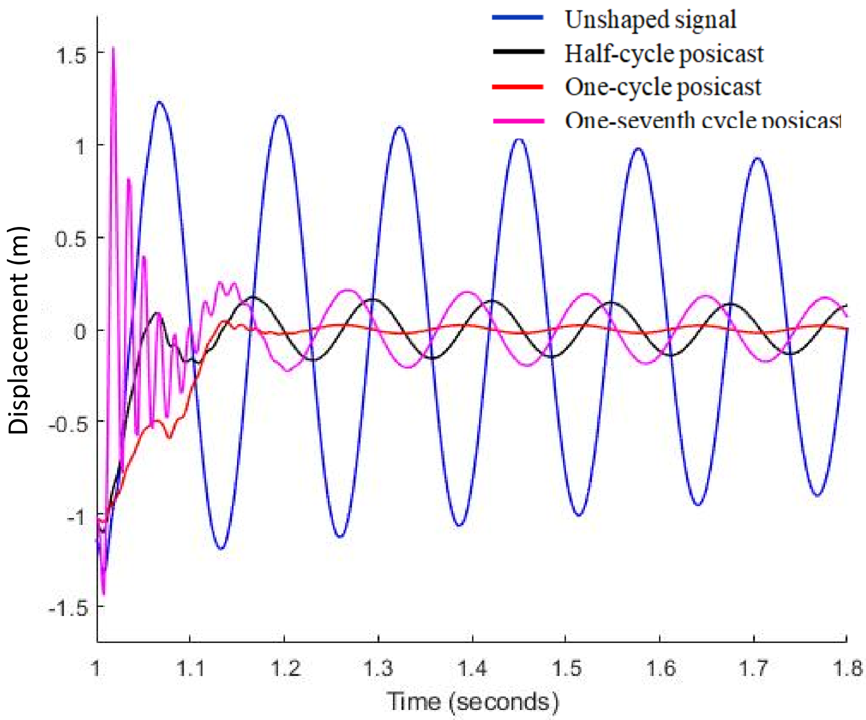

Figure 4.18 Comparison of the unshaped and the posicast controlled signals for TM-1 30°

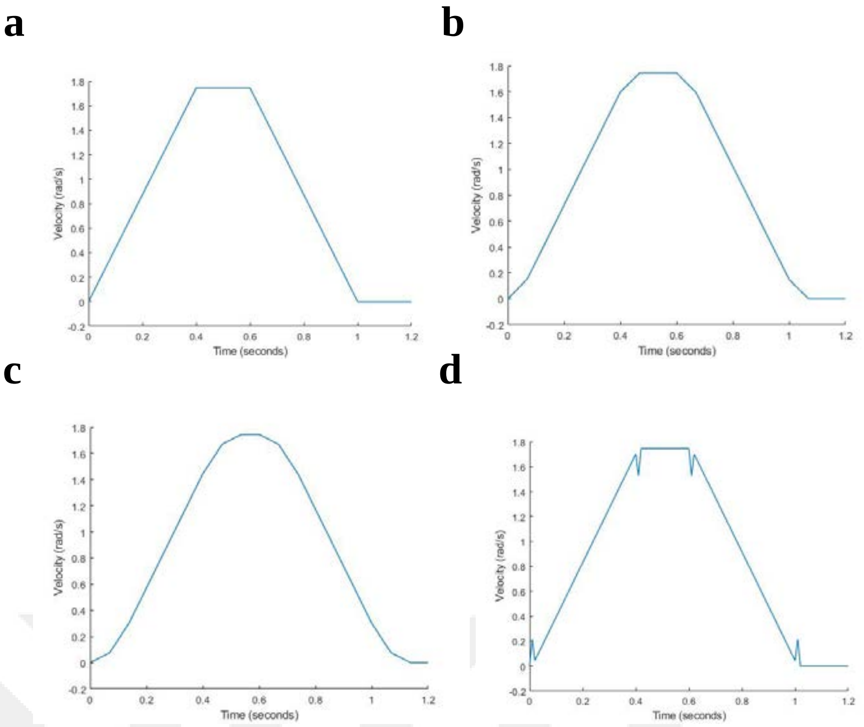

Figure 4.19 The input signals for TM-1 60° (**a** unshaped, **b** half-cycle, **c** one-cycle, **d** one-seventh cycle)

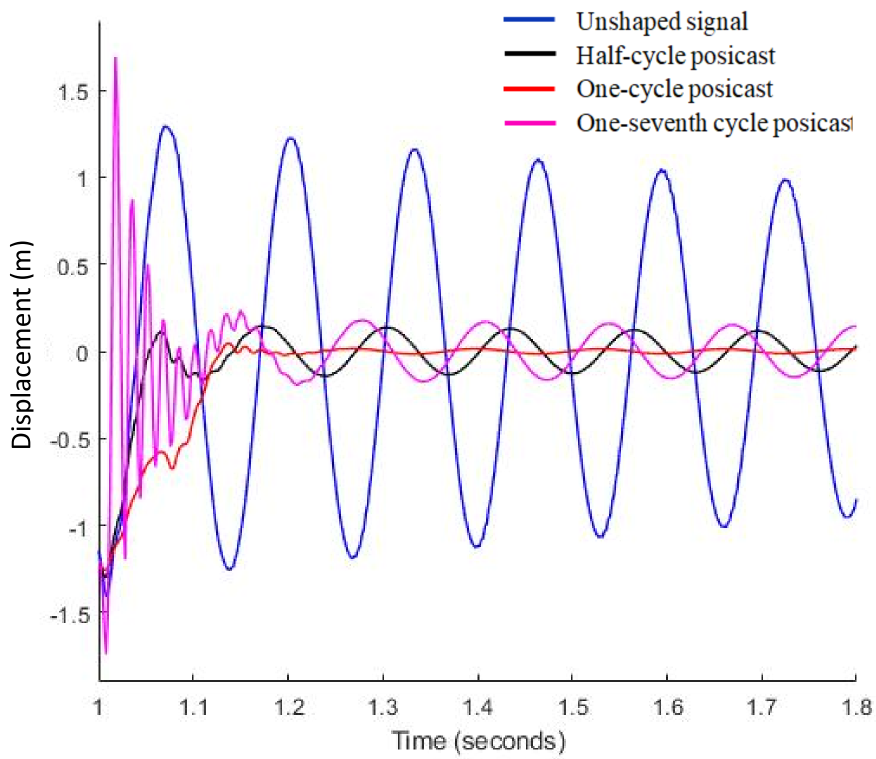

Figure 4.20 Comparison of the unshaped and the posicast controlled signals for TM-1 60°

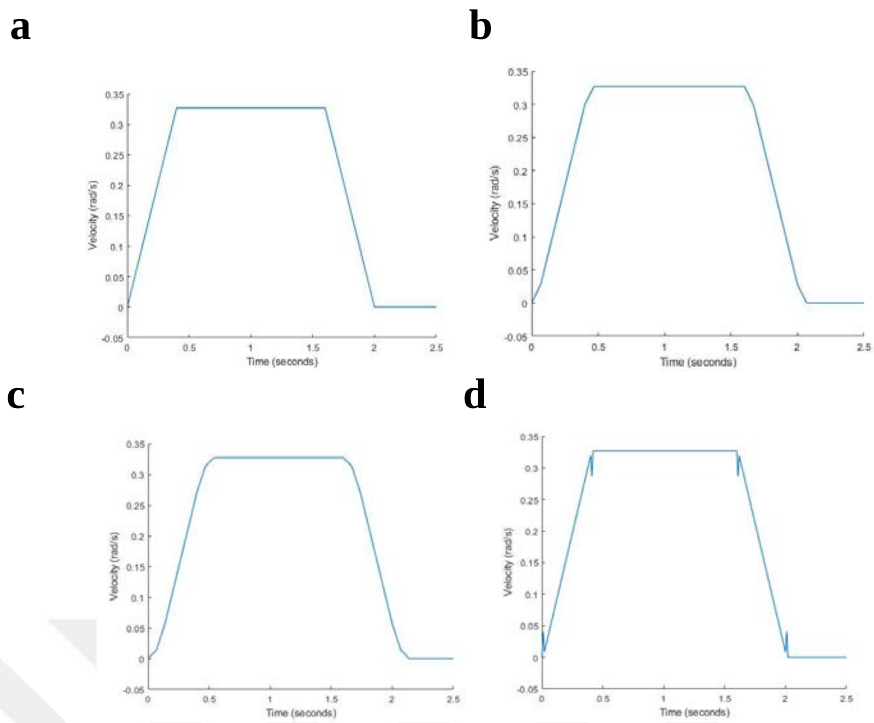

Figure 4.21 The input signals for TM-2 30° (**a** unshaped, **b** half-cycle, **c** one-cycle, **d** one-seventh cycle)

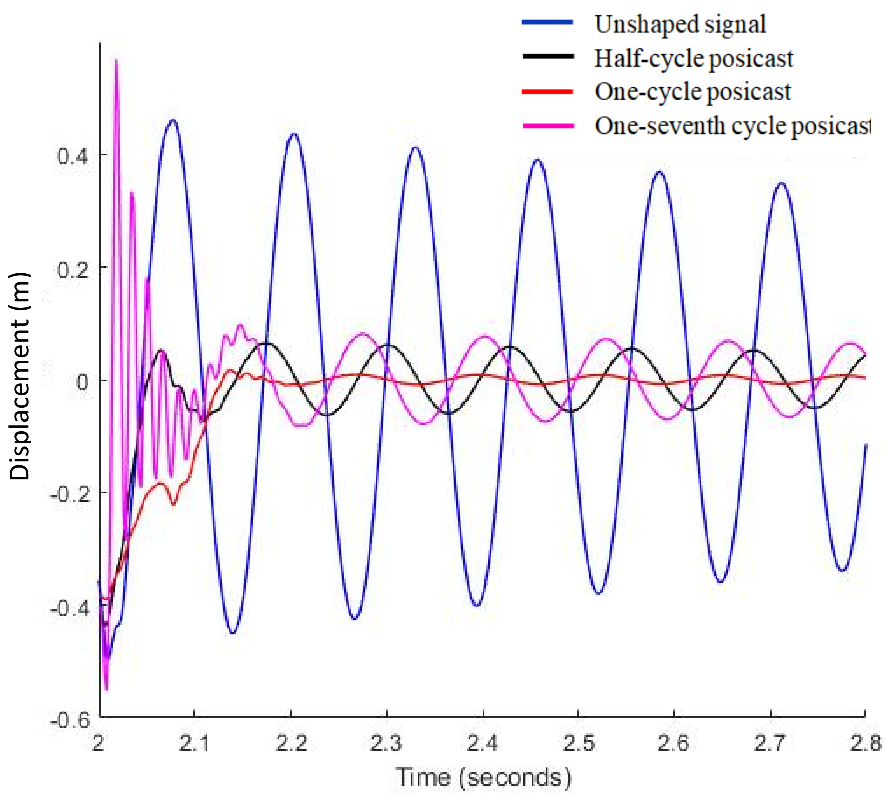

Figure 4.22 Comparison of the unshaped and the posicast controlled signals for TM-2 30°

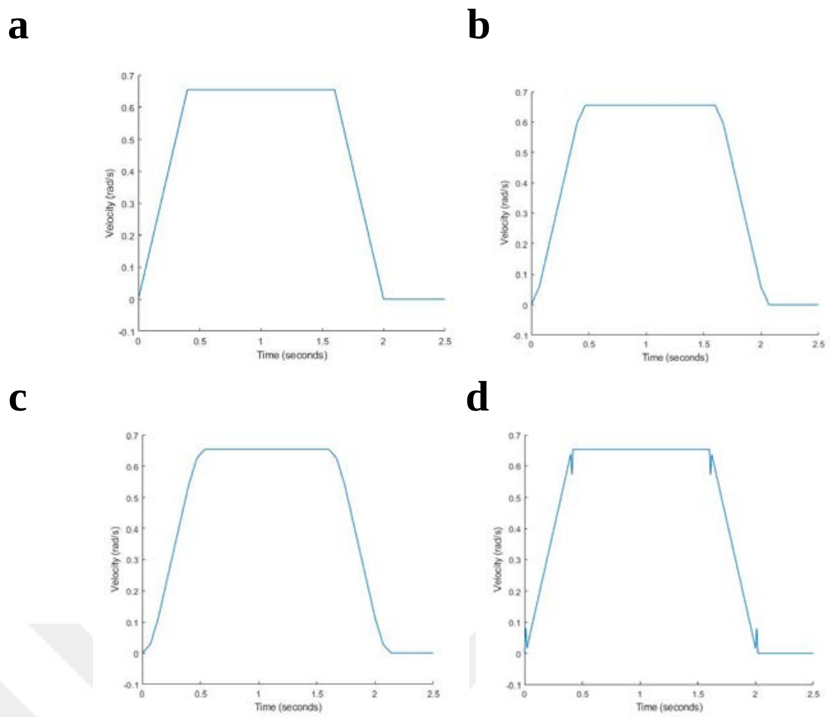

Figure 4.23 The input signals for TM-2 60° (**a** unshaped, **b** half-cycle, **c** one-cycle, **d** one-seventh cycle)

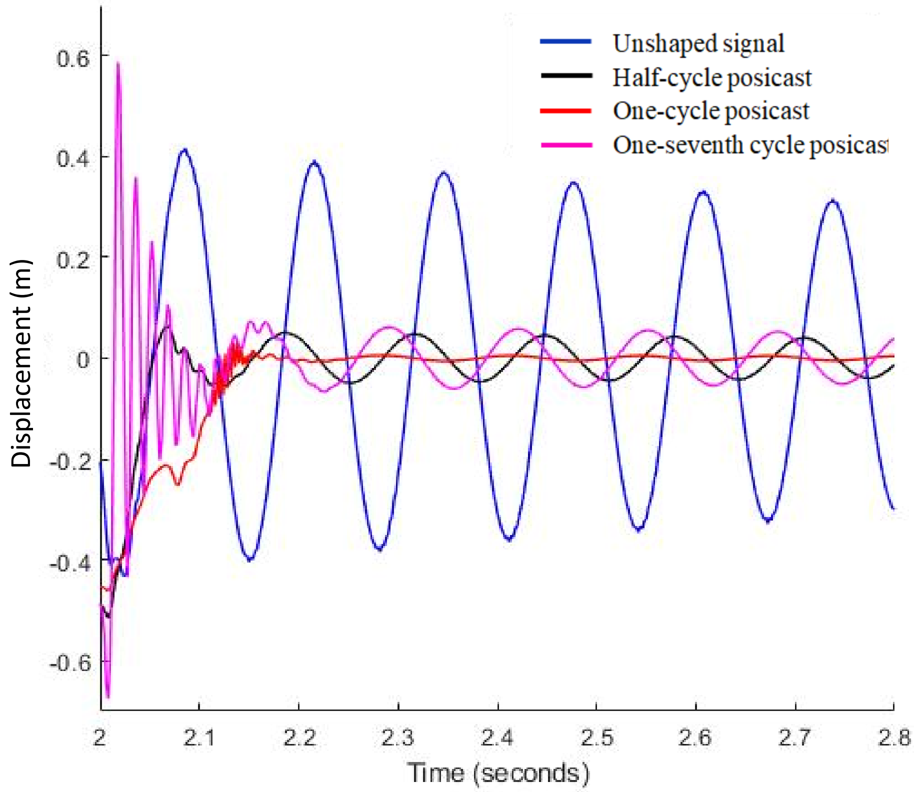

Figure 4.24 Comparison of the unshaped and the posicast controlled signals for TM-2 60°

In Table 4.3, the numerical values of the flexible planar manipulator are computed according to the motion angles 30° and 60°. During motion and residual vibration cases are determined as values of RMS. On the other hand, settling time is found. The cases and settling time are indicated for the each angle. For the unshaped and shaped results are given in Table 4.3 as numerical values.

Table 4.3 Results of the flexible planar manipulator system

TM-1

	30°			60°		
Posicast Types	**During Motion RMS (m)**	**Residual Vibration RMS (m)**	**Settling Time (s)**	**During Motion RMS (m)**	**Residual Vibration RMS (m)**	**Settling Time (s)**
Unshaped	1.194	0.2194	14.63	2.229	0.2377	15.55
Half-Cycle	0.9660	0.0311	10.21	1.7896	0.0271	10.36
One-Cycle	0.8749	0.0042	5.723	1.6244	0.003	5.165
One-third Cycle	0.9813	0.037	10.6	1.8159	0.0318	10.76
One-quarter Cycle	0.9983	0.0388	10.74	1.83	0.0332	10.89
One-fifth Cycle	1.012	0.0401	10.79	1.8453	0.0343	10.97
One-sixth Cycle	1.032	0.0414	10.81	1.8743	0.0346	10.96
One-seventh Cycle	1.068	0.0456	10.86	1.9352	0.0362	11.03

TM-2

	30°			60°		
Posicast Types	**During Motion RMS (m)**	**Residual Vibration RMS (m)**	**Settling Time (s)**	**During Motion RMS (m)**	**Residual Vibration RMS (m)**	**Settling Time (s)**
Unshaped	0.3621	0.0854	12.42	0.6560	0.0781	12.82
Half-Cycle	0.2582	0.0121	7.995	0.4592	0.0097	7.827
One-Cycle	0.2389	0.0016	3.511	0.4256	0.0011	2.635
One-third Cycle	0.2630	0.0144	8.392	0.4675	0.0113	8.223
One-quarter Cycle	0.2655	0.0151	8.518	0.4718	0.0119	8.361
One-fifth Cycle	0.2682	0.0156	8.582	0.4761	0.0122	8.437
One-sixth Cycle	0.2726	0.0157	8.584	0.4839	0.0124	8.439
One-seventh Cycle	0.2821	0.0161	8.658	0.5004	0.0130	8.501

As given in Table 4.3, the half-cycle posicast is demonstrated an efficient damping quality for all cases. The three-step cycles that are the one-cycle and the one-seventh cycle are compared to each other. The one-cycle is shown a robust damping quality. On the other hand, the one-seventh cycle is illustrated the lowest damping performance.

The half-cycle posicast is reduced RMS value from 1.194 to 0.966 in during motion-RMS in TM-1 30°. In the same motion position, residual vibration is decreased from 0.2194 to 0.0311 through the half-cycle posicast. The settling time is mitigated from 14.63 s. to 10.21 s. in TM-1 30°. RMS value is reduced from 2.229 to 1.7896 during motion in TM-1 60°. The residual vibration is decreased from 0.2377 to 0.0271 as RMS value in TM-1 60°. The settling time is diminished from 15.55 s. to 10.36 s. in TM-1 60°. The half-cycle posicast is realized reducing RMS value from 0.3621 to 0.2582 during motion in TM-2 30°. The residual vibration is decreased as RMS value from 0.0854 to 0.0121 through the half-cycle posicast in TM-2 30°. The half-cycle posicast is decreased from 12.42 s. to 7.995 s. to the settling time. In TM-2 60°, RMS value is mitigated from 0.656 to 0.4592 during motion. The half-cycle method is accomplished decreasing the residual vibration as RMS value from 0.0781 to 0.0097 in TM-2 60°. In addition, the settling time is mitigated from 12.82 s. to 7.827 s.

The one-cycle posicast is decreased RMS value from 1.194 to 0.8749 during motion in TM-1 30°. The one-seventh cycle posicast is reduced from 1.194 to 1.068. The residual vibration RMS value is mitigated from 0.2194 to 0.0042 in TM-1 30° through the one-cycle posicast. On the other hand, the one-seventh cycle posicast is reduced RMS value from 0.2194 to 0.0456. The one-cycle posicast is diminished the settling time from 14.63 s. to 5.723 s. in TM-1 30°. The one-seventh cycle posicast is determined reducing the settling time from 14.63 s. to 10.86 s. The one-cycle is decreased RMS value from 2.229 to 1.6244 during motion in TM-1 60°. The one-seventh cycle is reduced RMS value from 2.229 to 1.9352 during motion. The residual vibration is mitigated from 0.2377 to 0.003 as RMS value in TM-1 60° through the one-cycle. The one-seventh cycle is reduced RMS value from 0.2377 to 0.0362 in residual vibration-RMS in TM-1 60°. The settling time is decreased from 15.55 s. to 5.165 s. by the one-cycle posicast. The one-seventh cycle posicast is mitigated from 15.55 s. to 11.03 s. to the settling time in TM-1 60°.

In during motion, the one-cycle posicast is reduced RMS value from 0.3621 to 0.2389 in TM-2 30°. On the other hand, the one-seventh cycle is decreased from 0.3621 to 0.2821. The residual vibration RMS value is diminished from 0.0854 to 0.0016 by the one-cycle posicast. The one-seventh cycle posicast is demonstrated from 0.0854 to 0.0161 in the same motion position. In this position, the settling time is decreased from 12.42 s. to 3.511 s. by performing the one-cycle posicast. The one-seventh cycle posicast is succeed to reducing the settling time value from 12.42 s. to 8.658 s. in TM-2 30°. In during motion-RMS in TM-2 60°, the one-cycle posicast is applied to damping performance from 0.656 to 0.4256. On the other hand, the one-seventh cycle is decreased from 0.6560 to 0.5004. The residual vibration is reduced RMS value from 0.0781 to 0.0011 through the one-cycle posicast in TM-2 60°. The one-seventh cycle is reduced from 0.0781 to 0.0130 in the same motion position. The settling time is decreased from 12.82 s. to 2.635 s. by the one-cycle posicast. The one-seventh cycle posicast is realized diminishing from 12.82 s. to 8.501 s.

CHAPTER FIVE

CONCLUSIONS

In this study, the posicast control input shaping method is applied to the flexible systems for reducing residual vibrations. The flexible systems are investigated as the lumped-parameter systems and a planar manipulator. The systems are evaluated as three cases that are the during motion-RMS, residual vibration-RMS and settling time. The step and trapezoidal inputs are employed to the systems. The inputs are determined as two maximum velocities and two motion angles. The single and multi-degree-of-freedom spring-mass-damper systems are studied in MATLAB/Simulink. Furthermore, the flexible single-link planar manipulator is modelled and simulated in ANSYS. Shaped inputs are generated in MATLAB/Simulink for all system types. These studies show to conclusions the following:

- The posicast control method is an adaptive controller for step and trapezoidal input forms.

- Half-cycle and three-step cycle are utilized in this study. The three-step cycle comprises for forms of which from 1/1 cycle to 1/7 cycle.

- The results show that the one-cycle posicast is the most effective method in terms of reducing vibrations at both during motion time and residual vibration region.

- The half-cycle ensure better reduction than three-step cycle except for one-cycle form.

- In the S-DOF system, the half-cycle and one-third cycle offer similar efficiency.

- The settling times are almost zero for half-cycle, 1/1and 1/3 cycles in the S-DOF system. Generally, the settling times increase for the higher grade cycles of three-step method.

- Despite the higher velocities amplifies magnitudes of the response at the during motion time, the half-cycle and three-step cycle methods provides the vibration conrol, expectedly.

- The results of M-DOF system is compatible with the results of the manipulator system.

REFERENCES

Aghamohammadi, M. R., Ghorbani, A., & Pourmohammad, S., (2008). Enhancing transient and small signal stability in power systems using a posicast excitation controller. *In 2008 43rd International Universities Power Engineering Conference*, 1-5, IEEE.

Cook, G. (1966). An application of half-cycle Posicast. *IEEE Transactions on Automatic Control*, *11*(3), 556-559.

Cook, G. (1962). *Posicast versus conventional types of compensation in a control system* ([Doctoral dissertation], Massachusetts Institute of Technology).

Feng, Q., Hung, J. Y., & Nelms, R. M. (2003). Digital control of a boost converter using Posicast. In *Eighteenth Annual IEEE Applied Power Electronics Conference and Exposition*, *2003. APEC'03.* (Vol. 2, 990-995). IEEE.

Feng, Q., Nelms, R. M., & Hung, J. Y. (2006). Posicast-based digital control of the buck converter. *IEEE Transactions on Industrial Electronics*, *53*(3), 759-767.

Fowell, R. A. (1997, 11 March). Robust resonance reduction using staggered Posicast filters. *U.S. Patent No. 5,610,848*. Washington, DC: U.S. Patent and Trademark Office.

Ghorbani, H., Candela, J. I., Luna, A., & Rodriguez P. (2014). Posicast control—A novel approach to mitigate multi-machine power system oscillations in presence of wind farm. In *2014 IEEE PES General Meeting| Conference & Exposition,* 1-5. IEEE.

Ghorbani, A., Pourmohammad, S., & Ghazizadeh, M. S. (2008). Mitigation of oscillations due to changing the reference signal of the excitation system using a Posicast controller. In *2008 12th International Middle-East Power System Conference,* 57-61. IEEE.

Golnaraghi, F., & Kuo, B. C. (2017). *Automatic control systems*. McGraw-Hill Education.

Gonzalez, E. A. (2007). Posicast control in power electronics. In *Proceedings of the AUN/SEED-Net Fieldwise Seminar in Power Systems*, 21-22.

Hung, J. Y. (2003). Feedback control with posicast. *IEEE Transactions on industrial electronics*, *50*(1), 94-99.

Hung, J. Y. (2007). Posicast control past and present. *IEEE Multidisciplinary Engineering Education Magazine*, *2*(1), 7-11.

Kalantar, M., & Mousavi G. (2010), Posicast control within feedback structure for a DC DC single ended primary inductor converter in renewable energy applications, *Applied Energy* 87(10), 3110-3114.

Kucera, V., & Hromcik, M. (2011), Delay-based input shapers in feedback interconnections. *IFAC Proceedings Volumes*, *44*(1), 7577-7582.

Kuh, E. S. (1957). Synthesis of lumped parameter precision delay line. *Proceedings of the IRE*, *45*(12), 1632-1642.

Malgaca, L., Yavuz, Ş., Akdağ M., & Karagülle, H. (2016). Residual vibration control of a single-link flexible curved manipulator. *Simulation Modelling Practice and Theory*, *67*, 155-170.

Moura Oliveira, P. B., Pires, E. S., & Novais, P. (2015). Design of Posicast PID control systems using a gravitational search algorithm. *Neurocomputing*, *167*, 18-23.

Moura Oliveira, P. B., Vrančić, D., & Cunha, J. B. (2012, 16-18 July). Posicast PID control of oscillatory systems. In *10th Portuguese Conference on Automatic Control*, 16-18.

Oliveira, J., Oliveira, P. M., Pinho, T. M., & Boaventura-Cunha J. (2017, 3-6 July). Swarm-based auto-tuning of pid posicast control for uncertain systems. In *2017 25th Mediterranean Conference on Control and Automation (MED)* 1299-1303. IEEE.

Oliveira, P. M., & Vrančić, D. (2012). Underdamped second-order systems overshoot control. *IFAC Proceedings Volumes*, *45*(3), 518-523.

Park, S., Wee, D., Annaswamy, A. M., & Ghoniem, Ahmed F. (2002). Adaptive low-order posi-cast control of a combustor test-rig model. In *Proceedings of the 41st IEEE Conference on Decision and Control, 2002.* (Vol. 4, 3698-3703). IEEE.

Ribeiro, E. A., Pereira, J. T., & Bavastri, C. A. (2015). Passive vibration control in rotor dynamics: optimization of composed support using viscoelastic materials. *Journal of Sound and Vibration*, *351*, 43-56.

Rimašauskienė, R., Jūrėnas, V., Radzienski, M., Rimašauskas, M., & Ostachowicz, W. (2019). Experimental analysis of active–passive vibration control on thin-walled composite beam. *Composite Structures*, *223*, 110975.

Singh, T., & Singhose, W. (2002, 8-10 May). Input shaping/time delay control of maneuvering flexible structures. In *Proceedings of the 2002 American Control Conference (IEEE Cat. No. CH37301)* (Vol. 3, 1717-1731). IEEE.

Smith, O. J. (1957). Posicast control of damped oscillatory systems. *Proceedings of the IRE*, *45*(9), 1249-1255.

So, H. C., & Thaler, G. J. (1960). A modified posicast method of control with applications to higher-order systems. *Transactions of the American Institute of Electrical Engineers, Part II: Applications and Industry*, *79*(5), 320-326.

Sugiki, A., & Furuta, K. (2006), POSICAST control design for parameter-uncertain plants. In *Proceedings of the 45th IEEE Conference on Decision and Control*, 3192-3197. IEEE.

Tallman, G., & Smith, O. (1958), Analog study of dead-beat posicast control. *IRE Transactions on Automatic Control*, *4*(1), 14-21.

Tang, Z., Pan, Y., & Cheng, Z. (2019). Vibration analysis and passive control of SCARA robot arm. In *Proceedings of the 2019 International Conference on Robotics, Intelligent Control and Artificial Intelligence*, 89-93.

Tong, X., & Zhao, X. (2018). Passive vibration control of the SCOLE beam system. *Structural Control and Health Monitoring*, *25*(8), e2204.

Yavuz, Ş., Malgaca, L., & Karagülle, H. (2016). Analysis of active vibration control of multi-degree-of-freedom flexible systems by Newmark method. *Simulation Modelling Practice and Theory*, *69*, 136-148.

Yildiz Y., Annaswamy A., Kolmanovsky I. & Yanakiev D. (2010). Adaptive posicast controller for time-delay systems with relative degree $n* \leq 2$. *Automatica*, *46*(2), 279-289.

Younesian, D., Esmailzadeh, E., & Sedaghati, R. (2006). Passive vibration control of beams subjected to random excitations with peaked PSD. *Journal of Vibration and Control*, *12*(9), 941-953.